Inorganic Chemistry

Article

pubs.acs.org/IC

Introducing the 4-Phenyl-1,2,3-Triazole Moiety as a Versatile Scaffold for the Development of Cytotoxic Ruthenium(II) and Osmium(II) Arene Cyclometalates

Christoph A. Riedl,[†,‡] Lea S. Flocke,[†] Michaela Hejl,[†] Alexander Roller,[†] Matthias H. M. Klose,[†,‡] Michael A. Jakupec,[†,‡] Wolfgang Kandioller,*[,†,‡] and Bernhard K. Keppler[†,‡]

[†]Institute of Inorganic Chemistry, Faculty of Chemistry, and [‡]Research Platform "Translational Cancer Therapy Research", University of Vienna, Waehringer Strasse 42, 1090 Vienna, Austria

Supporting Information

ABSTRACT: Herein we report the synthesis, anticancer potency *in vitro*, biomolecule interaction, and preliminary mode of action studies of a series of cyclometalated 1,2,3-triazole-derived ruthenium(II) (**2a**–**e**) and osmium(II) (**3a**–**e**) organometallics of the general form [(η^6-*p*-cym)RuCl(κ^2-C^N-L)] with varying substituents in postion 1 of the 1,2,3-triazole moiety. These cyclometalates were characterized by standard analytical methods and their structures unambiguously assigned by single crystal X-ray crystallography. The anticancer activity of these novel compounds was tested in the human tumor cell lines A549 (non-small cell lung cancer), SW480 (colon adenocarcinoma), and CH1/PA-1 (ovarian teratocarcinoma), and preliminary structure–activity relationships were derived from the obtained data sets. Various representatives exhibit promising antineoplastic effects with IC_{50} values down to the low micromolar range. The compounds readily formed stable DMSO adducts after aquation in DMSO-containing solution, but employing DMSO as solubilizer in cytotoxicity assays had no pronounced effect on the cytotoxicity, compared to analogous experiments with DMF for most compounds. We isolated and characterized selected DMSO adducts as triflate salts and found that they show activities in the same range as the parent chlorido metalacycles in MTT assays with the use of DMSO. Osmium(II) cyclometalates exhibited higher antiproliferative activities than their ruthenium(II) counterparts. The IC_{50} values within each metal series decreased with increasing lipophilicity, which was attributed to higher cellular accumulation. Investigations on their mode of action revealed that the prepared organometallics were unable to inhibit topoisomerase IIα. Still, the most cytotoxic representatives **2b** and **3b** showed pronounced effects on cell cycle distribution.

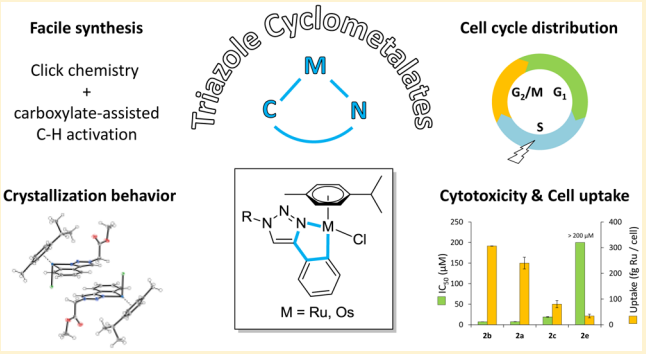

INTRODUCTION

Over the last decades, ruthenium-based metallodrugs have emerged as promising therapeutic agents in anticancer therapy. The first-in-class ruthenium(III) complex indazolium *trans*-[tetrachlorido-bis(*1H*-indazole)ruthenate(III)] (KP1019) has shown preclinical anticancer activity and a mild toxicity profile in a clinical phase I trial while eliciting disease stabilizations.[1] NKP-1339 or IT-139 (Figure 1), the sodium analog of KP1019, offers superior aqueous solubility and has successfully finished a clinical phase I trial with promising activity, especially in neuroendocrine tumors and non-small cell lung cancer.[2] The activation of Ru(III) agents by reduction to Ru(II) in the hypoxic tumor tissue is assumed to be essential in their mechanism of action.[3] Ruthenium(II) arene compounds offer a versatile framework for the development of novel anticancer agents, whose physicochemical, biological, and pharmacological properties can be readily modified by variation of the ligand sphere. Promising ruthenium(II) arene-based compound classes include 1,2-diaminoethane (en) complexes of the general form [Ru(η^6-arene)(en)X]$^+$ (X = halide) developed by Sadler and co-workers[4] and RAPTA compounds of the type [Ru(η^6-arene)(PTA)X_2] (PTA = 1,3,5-triaza-7-phosphaadamantane) established by the Dyson group.[5] Their investigations afforded the two promising anticancer agents RM175 and RAPTA-C, which are currently at an advanced preclinical stage (Figure 1).

Additionally, coordination of biologically active ligand systems to exploit synergistic effects has been a promising approach in recent years.[6] Both the scope of employed ligand systems, such as paullones,[7] flavonoids,[8] and naphtoquinones,[9] as well as the high antiproliferative activity of the derived complexes are impressive and continue to stimulate further research. Most ruthenium(II) arene compounds feature a halido leaving group and a bidentate *N,N*-, *N,O*-, *O,O*-, or *S,O*-chelating ligand. Replacement of the halido leaving group by a

Received: October 5, 2016

DOI: 10.1021/acs.inorgchem.6b02430
Inorg. Chem. XXXX, XXX, XXX–XXX

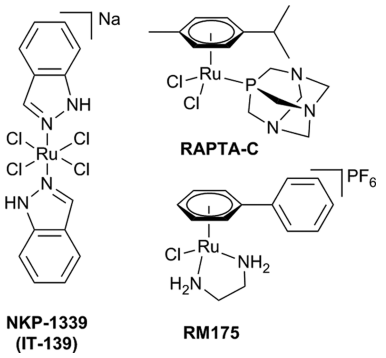

Figure 1. Promising ruthenium-based anticancer agents IT-139 (left), RAPTA-C (right, top), and RM175 (right, bottom).

water molecule is thought to be essential for the mechanism of action,[10] which is referred to as the activation-by-aquation hypothesis. However, poor stability of the bidentate coordination motif oftentimes hampers application of the respective organometallics as anticancer therapeutics,[11−13] which emphasizes the need to explore other coordination modes with altered properties. Over the last years, especially ruthenium(II) arene complexes bearing *C,N*-coordinating ligand systems have attracted considerable attention, and promising anticancer activities of cyclometalated 2-aryldiazole,[14] 2-phenylindole,[15] 2-phenylpyridine,[16] and benzimidazole[17,18] scaffolds have been reported.

Ruthena(II)cycles may be prepared by transmetalation from toxic organomercurated precursors, or more conveniently by carboxylate-assisted C−H activation.[19,20] While numerous examples of cytotoxic cyclometalated ruthenium(II) arene compounds can be found in the literature, osma(II)cycles seem to have been largely neglected. Ryabov and co-workers have reported and characterized osma(II)cycles of the form [Os(*p*-cym)(2-PhPy$_{C\wedge N}$)L] (L = Cl, MeCN; 2-PhPy = 2-phenylpyridine) as intermediates in the synthesis of [Os(II)-(chel)$_3$] metalacycles as electron carriers for active sites of oxidoreductases,[21−23] and *N*-pyridyl 1,2,3-triazolylidene ligand-bearing Os(II) metalacycles were explored for their applicability in transfer hydrogenation catalysis.[24] However, the biological properties and particularly the cytotoxicity of osma(II)cycles of the form [Os(arene)L$_{C\wedge N}$Cl] remain nearly unexplored and were only touched upon by Pfeffer and co-workers, who reported the promising cytotoxicity of [Os(*p*-cym)(2-PhPy$_{C\wedge N}$)Cl] in the low micromolar range.[25]

In order to expand the library of cyclometalated ruthenium-(II) and osmium(II) arene compounds, we turned to the highly versatile, robust, and extensively studied 1,2,3-triazole moiety. The discovery of the copper-catalyzed azide−alkyne cycloaddition (CuAAC) of an azide dipole and an alkyne dipolarophile for the regioselective synthesis of 1,4-disubstituted 1,2,3-triazoles independently by both Sharpless[26] and Meldal[27] in 2002 has led to a phenomenal rise in triazole-related research. The reaction is outstanding due to mild reaction conditions, high yield, facile workup, wide scope, and insensitivity to functional groups.[28] Convenient for medicinal applications, 1,2,3-triazoles possess high stability to metabolic degradation and hydrogen bonding capabilities to facilitate interaction with biological targets[29] while providing high variability by introduction of different substituents at positions 1 and 4. Through the straightforward variation of alkyne and azide substrates, the CuAAC reaction provides a robust pathway for the design of extensive ligand libraries and synthesis of diverse triazole-based coordination compounds.

Complexation of 1,4-disubstituted 1,2,3-triazoles to metal ions can occur at the N2- and N3-positions, of which the N3 atom possesses a higher Lewis basicity.[30] In contrast, alkylation at position N3 and subsequent deprotonation of the acidic C5−H proton allows monodentate coordination of the triazole ring as an abnormal mesoionic *N*-heterocyclic carbene (NHC).[31−33] Besides monofunctional coordination compounds, the facile introduction of donor functionalities through modified azide and alkyne CuAAC substrates has encouraged the development of bi- and multidentate triazole ligand systems. Nitrogen pendant donor functions such as 2-pyridyl residues[34] at position 4 or 2-picolyl substituents[35] at position 1 provide *N,N*-chelating moieties that readily form stable 5- or 6-membered chelate rings, respectively. Especially pyridyl-subsitituted triazoles (pytz), as well as the symmetrical 4,4′-bitriazolyl ligands (btz), have attracted considerable attention as bipyridine analogues for the design of photoactive complexes of ruthenium,[36−38] rhenium,[39] and iridium.[36,40] Similarly, cyclometalation of the aryl-1,2,3-triazole scaffold has also produced conveniently tunable photoactive complexes of ruthenium(II)[41] and iridium(III).[42] Furthermore, complexes featuring C^{NHC},*N*- or C^{NHC},C^{Ph}-coordination motifs have been explored for their catalytic activities.[43−46] In a recent investigation, organosulfur- or selenium-donor side chains allowed the synthesis of *S,N*- and *Se,N*-coordinated ruthenium(II) and palladium(II) complexes.[47]

Scheme 1. Synthesis of 1-Substituted 4-Phenyltriazole Ligands 1a−e, and Ruthenium(II) and Osmium(II) Arene Metalacycles 2a−e and 3a−e

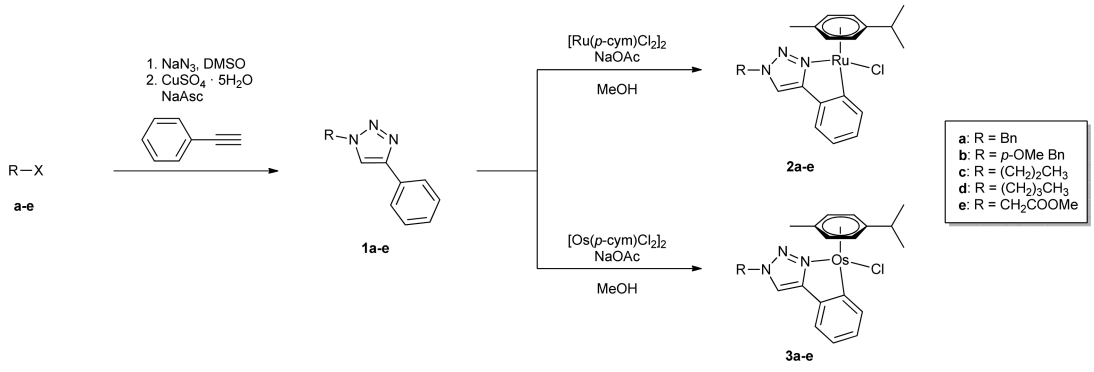

DOI: 10.1021/acs.inorgchem.6b02430
Inorg. Chem. XXXX, XXX, XXX−XXX

Intrigued by the possibilities for the implementation of bioactive functional groups and straightforward synthetic derivatization to explore structure−activity relationships, we aim to establish the cyclometalation of 1-substituted 4-phenyl 1,2,3-triazoles as a versatile motif for the development of novel ruthenium(II) and osmium(II) arene metallodrugs. In this work, we report the straightforward synthesis, characterization, and preliminary biological evaluation of a model series comprised of ruthena(II) and osma(II)cycles.

The impact of the substituents at position 1 of the triazole ring, the difference between ruthenium(II) and osmium(II) metal centers, and the choice of solubilizer for biological evaluations on the behavior in aqueous solution, interaction with biomolecules, antiproliferative activity, cellular accumulation, and cell cycle effects will be discussed.

RESULTS AND DISCUSSION

Synthesis. A series of five different 1-substituted 4-phenyl 1,2,3-triazoles (**1a−e**) featuring benzylic, aliphatic, or methyl ester residues R was synthesized via the CuAAC reaction. The required organic azides were prepared *in situ* by reaction of the respective organohalides with sodium azide in DMSO.[48] In order to avoid isolation of potentially explosive short-chained azides,[49] a one-pot CuAAC protocol was employed. Herein, the cycloaddition of organic azides in a mixture of water and DMSO (1:1) with phenyl acetylene is catalyzed by copper(I) generated *in situ* from copper(II) sulfate and sodium ascorbate.[50] After a reaction time of up to 24 h, the desired products **1a−e** were precipitated by addition of water and obtained in high purity and good to excellent (53−93%) yields (Scheme 1). Subsequently, a reliable cyclometalation procedure based on previous research was established. Kinetic investigations on the arylation of functional arenes by Jutand and co-workers[19,20] led to the formulation of a plausible mechanism for the carboxylate-assisted C−H activation.

First, the weakly bound monocoordinated acetate in the 18-e$^-$ complex [Ru(*p*-cym) $(OAc)_2$] is cleaved off, yielding a coordinatively unsaturated species, which enables coordination of the heterocyclic nitrogen. Subsequent formation of the *C,N*-coordinated metalacycle can be explained by deprotonation of the *ortho* C−H bond by uncoordinated acetate via an SE_3 mechanism.[51] The formed acetic acid accelerates the formation of the metalacycle by favoring the dissociation of acetate from [Ru(*p*-cym) $(OAc)_2$]; therefore, the reaction proceeds through an intermolecular deprotonation favored by carboxylate via an autocatalytic process. In their efforts to isolate the intermediate [Ru(p-cym)(2-$PhPy_{C\wedge N}$)(OAc)] by reaction of [Ru(*p*-cym)-$(OAc)_2$] with 2-phenylpyridine, Jutand and co-workers instead observed conversion to the chlorido complex. An authentic sample of [Ru(*p*-cym)Cl(2-$PhPy_{C\wedge N}$)] was obtained by reaction of $[Ru(p\text{-cym})Cl_2]_2$ with 2-PhPy in the presence of KOAc in acetonitrile at room temperature.[19]

Based on this research, we refined the complexation procedure for 1,2,3-triazole ligand systems. The target compounds were conveniently obtained by equimolar reaction of the respective ligand with the dimeric ruthenium(II) or osmium(II) arene metal precursor in the presence of sodium acetate (2.0 equiv) in anhydrous methanol. During the comparatively long reaction time of up to 48 h at room temperature, the product precipitates as a microcrystalline yellow solid. Under the chosen reaction conditions, no suitable substrate or sacrificial oxidant is present to exploit the activated metal−C(sp^2) bond, e.g. for direct arylation or homocoupling to form biaryl derivatives.[52] Subsequently, the transitional acetate complex [Ru(*p*-cym)($trz_{C\wedge N}$)(OAc)] undergoes a ligand exchange to the more favorable chlorido complex,[19] which precipitates from the reaction solution. Acceptable reaction times are achieved only with high concentrations of triazole ligands and metal dimer in the reaction solution.

However, neither increased reaction temperatures, microwave irradiation, higher acetate catalyst, nor additional acetic acid cocatalyst loadings could accelerate the reaction rate. The precipitated product was collected by filtration, washed with methanol to remove impurities, then redissolved in dichloromethane and filtered to remove inorganic salts. Evaporation to dryness afforded the desired metalacyles in elemental analysis purity and moderate to good yields (52−81%). Recently, a similar procedure was published by the Dixneuf group, which has to rely on chromatographic purification.[53]

Characterization. The isolated compounds were characterized by standard analytical methods such as ^1H, ^{13}C and 2D NMR, high-resolution ESI-mass spectrometry, X-ray crystallography, and elemental analysis.

Upon metal coordination, the rotational symmetry of the 4-phenyl ring is broken, which affords the characteristic coordination motif of two doublets and two doubletic doublets in ^1H NMR spectra, which were utilized to confirm the conversion. The aryl proton *ortho* to the metalated carbon is significantly shifted downfield and found around 8.15 ppm (Ru^{II}) and 8.01 ppm (Os^{II}) due to the electron withdrawing effect of metal coordination.

Additionally, coordination of the triazole ligand hinders inversion at the metal center in aprotic $CDCl_3$. As a consequence, the arene protons of *p*-cymene can be observed as four non-equivalent doublets, while the diastereotopic methylene proton of the triazole substituents in position 1 are split into two distinct doublets with a germinal coupling constant between 15 and 18 Hz.

The high-resolution ESI mass spectra of the ligands **1a−e** are dominated by the monomeric and dimeric sodium adducts $[M+Na]^+$ and $[2M+Na]^+$, while the proton adducts $[M+H]^+$ are observed as the least intense peak. The metal complexes **2a−e** and **3a−e** are found both as sodium adduct $[M+Na]^+$, as well as chlorido abstracted species $[M-Cl]^+$. Additionally, the osmium(II) complexes are observed as dimeric sodium adducts $[2M+Na]^+$.The intensity of these peaks varies greatly between compounds and is seemingly uncorrelated to their structures. This can be explained by a varying degree of chlorido leaving group hydrolysis due to different times between sample preparation and measurement in the chosen solvent system (MeCN:MeOH = 1:1, +1% H_2O).

The structures of the synthesized metalacycles were unambiguously confirmed by X-ray crystallography. Single crystals of **2a−e** and **3a−e** suitable for X-ray diffraction analysis were obtained by slow diffusion of *n*-hexane or diethyl ether into dichloromethane or chloroform complex solutions (Figure S5−S14). For detailed crystal data, data collection parameters, structure refinement details, and CCDC codes, please refer to the Supporting Information. Selected bond lengths, bond angles, and torsion angles are listed in Table S3−S6. These half sandwich complexes adopt the pseudotetrahedral "piano-stool" configuration, with the π-bonded *p*-cymene ligand acting as "seat", while the cyclometalated triazole ligand and chlorido leaving group formally act as "legs" (Table S2, Figure S1).

The benzyl (**2a**, **2b**, **3b**) and ester (**2e**, **3e**) derivatives are representatives of the triclinic space group $P\bar{1}$, while complexes

DOI: 10.1021/acs.inorgchem.6b02430
Inorg. Chem. XXXX, XXX, XXX−XXX

featuring either propyl (**2c**, **3c**) or butyl (**2d**, **3d**) side chains crystallize in the tetragonal space group $I4_1/a$. In contrast, the benzyl derivative **3a** crystallizes in the monoclinic $P2_1/n$ space group, supposedly due to incorporation of a dichloromethane solvent molecule into the crystal lattice, which also leads to increased ellipsoids through thermal oscillation.

The crystal lattices of **2b**−**e** and **3a**−**e** are populated with dimeric building blocks containing one (*R*) and one (*S*)-configured isomer of these chiral-at-metal metalacycles. As a result of cyclometalation, the phenyl and triazole rings are locked in plane, as can be seen from the low torsion angles between 0.6(6)° to 4.4(8)° along the triazole−phenyl bond. The coplanar triazole and phenyl rings of the dimeric pairs are arranged in parallel layers, with the chlorido ligands pointing toward the interaction partner, while the bulky isopropyl group of the arene ring residing at position 1 is rotated toward the backside of the plane (Figure 2) due to hydrophobic interactions.

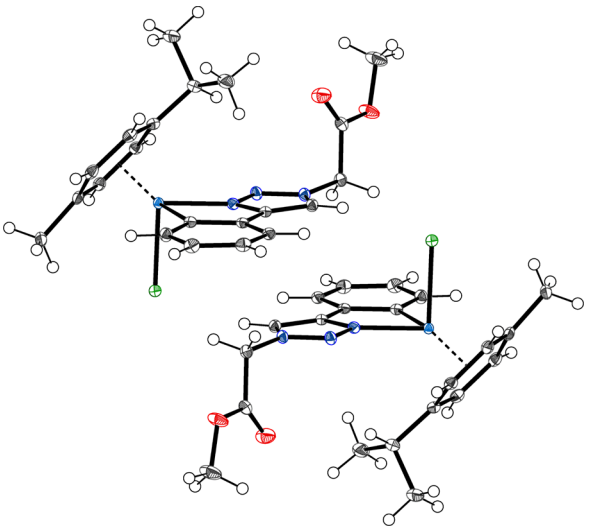

Figure 2. Interaction pair of **2e** as an example of dimeric subunits.

The driving force for the parallel assembly is likely $\pi-\pi$ stacking between the 4-phenyl triazole rings. The observed centroid−centroid distances range from 3.6 to 4.0 Å with a displacement angle from 23 to 31°. Typical parallel-displaced π stacking interaction is reported to occur in centroid distances up to 3.8 Å and angles around 20°.[54] The slightly increased offset in the 4-phenyl triazole-based organometallics can be explained by intermolecular $\pi_{trz}-\sigma_{trz\text{-}H}$ attraction and in some cases $\pi_{Ph}-\sigma_{CH2}$ attraction between side chain protons and the phenyl ring (Figure S3, Table S7−S9).

The far order of the dimeric subunits is determined by the side chains. The tetragonal alkyl derivatives **2c**, **2d**, **3c**, and **3d** arrange themselves in orthogonal layers (Figure S2, left) in order to minimize energy by aggregation of lipophilic alkyl chains and comparatively polar metal centers. In most benzyl and ester derivatives (**2b**, **2e**, **3a**, **3b**, **3e**), the triazole and phenyl rings are locked in parallel plains (Figure S2, right). In crystals of **2a** the individual molecules arrange themselves in long parallel chains rather than the dimeric interaction pairs discussed above, facilitated by alternating π-interactions between the triazole and phenyl rings of consecutive molecules ($\pi_{trz(a)}-\pi_{Ph(b)}$, $\pi_{trz(b)}-\pi_{Ph(c)}$, etc.; Figure S4).

The metal−chlorido bond lengths were found to be between 2.4165(17) and 2.4320(14) Å, a typical range for organometallic ruthenium[55,56] and osmium[57,58] complexes. The metal−N and metal−C bonds range from 2.069(6) to 2.088(4) Å, and 2.057(6) to 2.096(5) Å, respectively. Slightly shorter metal−arene distances were found in all osmium complexes, except **3e**, compared to their ruthenium counterparts. Metal coordination distorts the phenyl ring, thereby significantly shortening bonds emanating from the metalated carbon, and elongating the remaining C−C bonds of the phenyl ring, which can be attributed to the electron withdrawing effect of coordination. Additionally, the phenyl ring is bent toward the triazole N2, as can be seen in the decreased $C_{Ph}-C_{trz\text{-}4}-N_{trz\text{-}3}$ bond angle from 115.11(10) to 113.8(7)° in the complexes compared to the free ligand with 122.8° (Table S5).

Stability in aqueous solution. All biological investigations were performed with the help of a solubilizing agent such as DMSO or DMF in order to compensate the limited aqueous solubilities of the developed compounds. UV−vis spectra of the complexes (20 μM, 1% solubilizer/67 mM phosphate buffer pH 7.4) were recorded over 24 h to determine the stability of the synthesized metalacycles under pseudophysiological conditions (Figure S15−S24). In 1% DMF, the initially clear solutions of ruthenium(II) and osmium(II) complexes undergo slight precipitation over time, which results in an overall decrease of absorption without the emergence of new peaks, shift of peak maxima, or occurrence of isosbestic points. In contrast, most compound spectra in 1% DMSO undergo a small shift of the peak maxima after the first measurement, yet afterward, the absorption over the whole wavelength range remains constant without the microprecipitation observed in DMF. In order to rule out interaction of the employed phosphate buffer with the organometallics, ^{1}H and ^{31}P NMR spectra of **2e** and **3e** in 10% d_6-DMSO or d_7-DMF and phosphate-buffered D_2O were recorded over 24 h. No spectral change or emergence of new peaks in ^{31}P spectra compared to reference spectra without cyclometalates was observed over the experiment time (Figure S25−S28). Additionally, the respective ^{1}H spectra showed the same changes over time as unbuffered samples, suggesting that interaction of phosphate buffer with the metal compounds does not cause the change in UV−vis spectra.

Recently, Gasser and co-workers presented a systematic study of the in-solution displacement of κN-monodentate bound ligands by DMSO in stock solutions of Ru^{II} organometallic complexes of the form [Ru(η^6-arene)(X)(Y)(Z)].[59] It was proposed that coordination and dissociation of the monodentate organic ligand occurs as an equilibrium reaction and is mainly influenced by the properties of the organic moiety. Complexes featuring ligands prone to dissociation in DMSO stock solutions self-evidently exhibit altered properties in biological screening when tested from DMSO stock solutions.

Consequently, DMSO-mediated complex dissociation is essential to be investigated prior to the biological experiments of the bidentate triazole-derived metalacycles presented in this work. Due to the suspected greater stability of bidentate coordination motifs, we propose exchange of the chlorido ligand with DMSO to be the cause of the spectral change in UV−vis investigations of **2a**−**e** and **3a**−**e**.

To further investigate this behavior, 5 μM complex solutions in 1% DMSO/400 μM ammonium acetate solution (5 μM, pH 7.4) were incubated at 37 °C; samples were taken after 0, 1, 3, 6, and 24 h and analyzed via ESI-MS after dilution with

DOI: 10.1021/acs.inorgchem.6b02430
Inorg. Chem. XXXX, XXX, XXX−XXX

methanol. Over the whole time span, only DMSO adducts $[M-Cl+DMSO]^+$ were observed, confirming the proposed leaving group exchange (Figure S29).

On the contrary, in 1% DMF/ammonium acetate solution only the molecular ion [M−Cl] was observed, whose peak height decreased over time by precipitation from solution, but also by decomposition yielding the mixed hydroxido/methoxido ruthenium dimers $[(p\text{-cym})Ru(OH)_m(OMe)_nRu(p\text{-cym})]$ (m + n = 3, Figure 3).

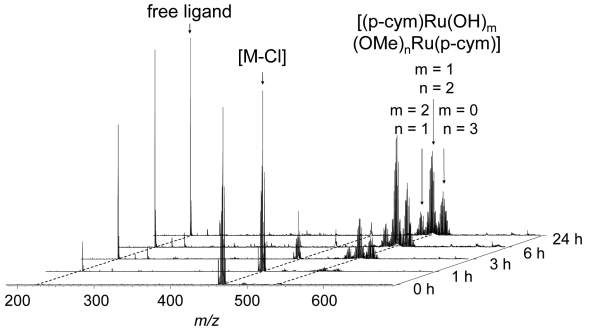

Figure 3. ESI-MS spectra of **2a** (5 μM) in 1% DMF/ammonium acetate solution (400 μM, pH 7.4) measured after 0, 1, 3, 6, and 24 h of incubation time at 37 °C.

Aquation−anation equilibria. The aquation−anation equilibria of **2e** and **3e** were studied by recording the ^{1}H NMR spectra of 500 μM compound solutions in 10% d_7-DMF/D_2O at 25 °C, both without NaCl and in the presence of 5 mM or 154 mM NaCl as model conditions for intra- and extracellular chloride concentrations.

The chlorido species and the derived aquated complex reach equilibrium concentrations after approximately 30 min (**2e**, Figure S31) and 90 min (**3e**, Figure S32), respectively.

The equilibrium concentrations are influenced by the chloride concentration in solution (Table 1), with almost

Table 1. Equilibrium Aquation−Anation Ratio

	Equilibrium aquation [%]		
Compound	0 mM NaCl	5 mM NaCl	154 mM NaCl
2e	95	85	25
3e	98	78	9

complete hydrolysis in pure water, slightly decreased hydrolysis in intracellular chloride concentrations (5 mM NaCl), and significantly hindered aquation under extracellular conditions (154 mM NaCl). This behavior suggests that a larger portion of the compound may enter the cell intact and subsequently undergo aquation in close proximity to the cellular targets. As to be expected, the rate of aquation is significantly slower in osmium(II) complexes than their ruthenium(II) counterparts, which may influence their biological effects.[60,61]

It has to be noted that slight precipitation of **2e** in 154 mM NaCl solution, and of **3e** under all NaCl concentrations was observed. Addition of sodium chloride to a completely hydrolyzed sample of **2e** and **3e** shifted the reversible aquation−anation equilibrium back toward the chlorido complex. However, a strong excess of sodium chloride induced quantitative precipitation (Figure S33), as previously reported for structurally related metalacycles.[17]

Solutions of all organometallics **2a−e** and **3a−e** in d_7-DMF and d_6-DMSO containing adventitious water showed no sign of decomposition, adduct formation, or hydrolysis in ^{1}H NMR over several days, which allowed easy handling of stock solutions for biological assays. Even upon addition of 10% D_2O, only slight formation of the aquated complex (DMF) and the DMSO adduct (DMSO) was observed (<5%, **2e**) overnight. Formation of the DMSO adducts in 10% DMSO/water proceeded with the same rate in pure water and physiological chloride concentrations (0.9% NaCl). Furthermore, no set of signals corresponding to the aquated species was observable in ^{1}H NMR, which suggests that aquation is the rate-determining step for DMSO adduct formation.

Amino acid interaction. The reactivity of the synthesized metalacycles toward amino acids was investigated by incubating 5 μM solutions containing of **2a−e** and **3a−e** with equimolar amounts of L-histidine (His), L-methionine (Met), and L-cysteine (Cys) in 1% DMF or DMSO/ammonium acetate solution (400 μM, pH 7.4). After 0, 1, 3, 6, and 24 h, aliquots were taken and analyzed by ESI-MS.

In 1% DMF the aquated metalacycles readily formed amino acid adducts, preferably with Met, to a lesser degree with His, and barely detectable with Cys (Figure 4). After 6 h, only

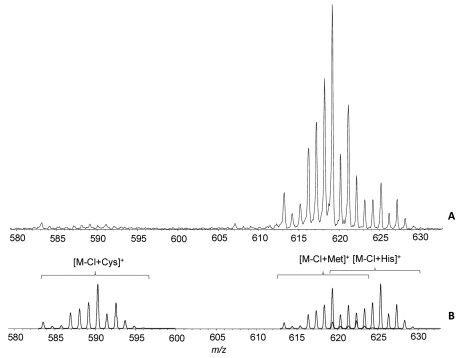

Figure 4. (A) ESI-MS spectrum of **2a** (5 μM) after 24 h of incubation with equimolar amounts of His, Met, and Cys; (B) calculated isotopic distributions of amino-acid adducts of **2a**: $[M-Cl+Cys]^+$, $[M-Cl+Met]^+$, and $[M-Cl+His]^+$.

amino acid adduct peaks were observed in mass spectra of all ruthena(II) and osma(II) cycles. In 1% DMSO-containing solutions, the only observable metal-containing peak corresponded to the DMSO adduct $[M-Cl+DMSO]^+$ (Figure S30), attesting to the strength of the DMSO-Ru bond.

Cytotoxicity. The antiproliferative activity of the ligands **1a−e** and the respective ruthenium **2a−e** and osmium **3a−e** complexes in human non-small cell lung cancer (A549), colon adenocarcinoma (SW480), and human ovarian carcinoma (CH1/PA-1) cell lines were determined by means of the colorimetric MTT assay. As could be seen from studies on interactions with small biomolecules, the *in situ* formed DMSO adducts showed no interactions with nucleophiles in contrast to the aqua complex. As the reactivity of the aqua species toward nucleophiles is postulated to be essential for the cytotoxic effect (activation-by-aquation hypothesis),[62] DMSO adduct formation should have an impact on anticancer potency. However, prescreens did not reveal major differences in activities with the use of DMSO or DMF as a solubilizer. Therefore, we were compelled to investigate the antiproliferative activity of the

DOI: 10.1021/acs.inorgchem.6b02430
Inorg. Chem. XXXX, XXX, XXX−XXX

prepared organometallics in DMSO- and DMF-containing cytotoxicity assays.

The free triazole ligands **1a−e** were tested from DMSO stocks with effective maximum contents of 0.5% v/v DMSO in the test plates, but IC_{50} values were not reached with soluble concentrations (**1a**, **1b**) or with concentrations of up to 200 μM (**1c−e**), except for **1a** in CH1/PA-1 (Table 2).

Table 2. 50% Inhibitory Concentrations (means ± standard deviations) of the Free Triazole Ligands 1a−e with DMSO as a Solubilizer in Three Human Cancer Cell Lines

	IC_{50} (μM)		
Compound	A549	SW480	CH1/PA-1
1a	>80	>80	62 ± 2
1b	>50	>50	>50
1c	>200	>200	>200
1d	>200	>200	>200
1e	>200	>200	>200

The prepared complexes **2a−e** represent the first examples of Ru^{II}(cym)triazoles with a C^{Ph},N^{3}-chelation motif. In contrast to the free ligands, the ruthenacycles **2a−c** exhibited considerable cytotoxic effects with IC_{50} values down to the low micromolar range for complexes **2a** and **2b**. In general, the complexes were most active in the chemosensitive CH1/PA-1 cell line. The antiproliferative potential of the investigated ruthenium complexes was found in the same range as the most active reported ruthenacycles of the general formula [Ru^{II}(arene)-($L^{C\wedge N}$)], such as cyclometalated 2-aryldiazole (10−150 μM),[14] 2-phenylindole (0.7−5 μM),[15] 2-phenylpyridine (3−100 μM),[16] and benzimidazole (1−150 μM)[17,18] scaffolds.

However, comparison of the cytotoxicities determined here with literature reports of other *C,N*-cyclometalates measured in different cell lines is not straightforward, and the observed IC_{50} values can therefore only give an estimate of the cytotoxicity relationships within each compound series.

In contrast to several reports on the anticancer potential of [Ru^{II}(arene)($L^{C\wedge N}$)] ruthenacycles, the respective Os(II) analogs were rather sparse in the literature. In this study, the prepared Os(II) complexes **3a−e** were found to be significantly more cytotoxic than the corresponding ruthenated complexes of the same ligand (Table 3) by factors of around 2−4 depending on the cell line and ligand. Like in the ruthenium series, the Os(II)(cym) complexes **3a** and **3b** bearing a pendant benzyl group at the N1 of the triazole backbone were found to be the most active of the series. The presented cytotoxicity data for the osmium(II) arene cyclometalates **3a−e** enable the first broader comparison of Os(II) arene complexes bearing *C,N*-coordinated 4-phenyl 1,2,3-triazoles to their ruthenium(II) congeners.

Organometallics derived from benzyl-substituted triazole ligands show the highest cytotoxic potency, especially in the chemosensitive CH1/PA-1 cells. Methyl ester-bearing triazole organometallics **2e** and **3e** exhibit the lowest cytotoxicity over all tested cell lines, with a more than 3- to 6-fold decreased activity depending on the cell line, compared to the most active representatives. Introduction of a methoxy group in benzyl derivatives and elongation of the alkyl chain only have a minor effect on IC_{50} values.

In order to elucidate the reason for the divergent IC_{50} values within the ruthenium(II) and osmium(II) metalacycle series, the cellular accumulation of selected ruthenium(II) compounds was measured in SW480 cells. Cellular accumulation is highest for the comparatively lipophilic benzyl residue compounds **2a** and **2b**, slightly lower for the alkyl derivative **2c**, and lowest for the metalacycle **2e**, featuring the least lipophilic methyl ester-bearing ligand **1e** (Table 4).

Table 4. Cellular Accumulation in SW480 Cancer Cells (0.5% DMSO, 50 μM compound), and Calculated Log*P* Values of the Corresponding Free Ligands (Molinspiration)

Compound	Cell uptake (fg Ru/cell)	cLog*P* (free ligand)
2a	240 ± 46	3.12
2b	306 ± 1	3.18
2c	80 ± 28	2.40
2e	34 ± 3	1.39

Increased cellular accumulation correlates well with lower IC_{50} values (Figure 5), which suggests that chain variation mainly impacts the antiproliferative abilities by modulation of the lipophilicity and presumably does not contribute additional interactions.

As far as the differences associated with the use of different solubilizers (DMSO vs DMF) are concerned, the benzyl and alkyl residues bearing ruthena(II)- and osma(II)cycles mostly exhibit antiproliferative activities in a comparable range. The

Table 3. 50% Inhibitory Concentrations (means ± standard deviations) of the Ruthenium and Osmium Arene Organometallics 2a−e and 3a−e in Three Human Cancer Cell Lines

	Solubilizer: DMF			Solubilizer: DMSO		
Compound	A549	SW480	CH1/PA-1	A549	SW480	CH1/PA-1
2a	16 ± 2	6.8 ± 0.1	5.7 ± 0.1	13.7 ± 0.3	7.3 ± 0.4	4.3 ± 0.9
2b	13 ± 1	6.6 ± 0.1	4.6 ± 0.7	13.7 ± 0.3	7.1 ± 0.1	4.0 ± 0.6
2c	>50	30 ± 4	15 ± 3	23.2 ± 0.3	19 ± 1	8.8 ± 0.7
2d	>12.5	>12.5	10 ± 2	>12.5	11.0 ± 0.2	6.1 ± 1.3
2e	109 ± 10	37 ± 3	16 ± 3	>200	>200	61 ± 14
3a	6.0 ± 0.4	3.6 ± 0.1	0.98 ± 0.20	12 ± 2	7.7 ± 0.8	1.4 ± 0.3
3b	5.5 ± 0.6	3.6 ± 0.1	1.2 ± 0.2	9.8 ± 2.0	6.0 ± 1.0	1.20 ± 0.01
3c	17 ± 1	11 ± 1	2.0 ± 0.2	43 ± 2	20 ± 2	4.1 ± 1.3
3d	7.7 ± 0.2	6.8 ± 0.5	1.5 ± 0.2	Insufficient solubility		
3e	34 ± 2	20 ± 1	3.3 ± 0.7	>50	>50	33 ± 13
cisplatin[63,a]	6.4 ± 0.4	3.3 ± 0.2	0.077 ± 0.006	6.4 ± 0.4	3.3 ± 0.2	0.077 ± 0.006

[a]Tested without the use of a solubilizing agent.

DOI: 10.1021/acs.inorgchem.6b02430
Inorg. Chem. XXXX, XXX, XXX−XXX

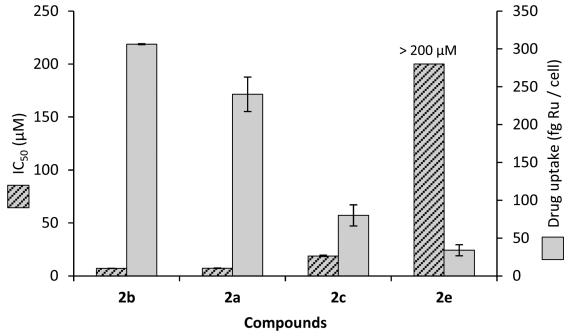

Figure 5. IC_{50} values (hatched) and cellular accumulation (plain) of **2a–d** in SW480 cells.

largest decrease in activity by the use of DMSO is found for methyl ester functionalized compounds **2e** and **3e**.

To investigate this behavior, we developed a procedure to isolate selected DMSO adducts **2a′**, **2e′**, and **3e′** as triflate salts based on chlorido ligand abstraction with silver triflate and reaction with DMSO in THF, and determined their cytotoxic activity (Table 5).

Table 5. 50% Inhibitory Concentration (mean ± standard deviation) of Cancer Cell Growth in Three Cell Lines Obtained by the MTT Assay with either DMSO (I) or DMF (II) as Solubilizer

	IC_{50} (μM)		
Compound	A549	SW480	CH1/PA-1
2a^{I}	13.7 ± 0.3	7.3 ± 0.4	4.3 ± 0.9
2e^{I}	>200	>200	61 ± 14
3e^{I}	>50	>50	33 ± 13
2a^{II}	16 ± 2	6.8 ± 0.1	5.7 ± 0.1
2e^{II}	109 ± 10	37 ± 3	16 ± 3
3e^{II}	34 ± 2	20 ± 1	3.3 ± 0.7
2a′^{II}	14 ± 1	8.4 ± 0.3	3.8 ± 0.5
2e′^{II}	>200	140 ± 9	43 ± 12
3e′^{II}	>200	>200	117 ± 5

The antiproliferative activity of the isolated DMSO adducts **2a′**, **2e′**, and **3e′** is remarkably close to those of the parent chlorido-bearing metal complexes **2a**, **2e**, and **3e** tested from DMSO stocks (Table 5). This suggests that the DMSO adducts may contribute to the antiproliferative effect measured in MTT assays.

While no biomolecule interaction of the *in situ* formed DMSO adducts could be observed via ESI-MS methods as discussed, the stability of the metal–DMSO bond may be different under extra- and intracellular conditions, thereby allowing for the formation of reactive species and a reaction with amino acids and other cellular targets.

As mentioned above, the use of either DMSO or DMF as a solubilizer has only a minor effect on the IC_{50} values of benzyl and alkyl derivatives **2a–d** and **3a–d**, while the methyl ester compounds **2e** and **3e** experience a large decrease in activity due to DMSO coordination. Through replacement of the chlorido ligand by DMSO, charged metal complexes with increased hydrophilicity are formed. It can be hypothesized that the already comparatively hydrophilic metalacycles **2e** and **3e** are unable to enter the cells to a sufficient degree upon DMSO coordination, which should diminish the antiproliferative activity. On the other hand, the DMSO adducts of more apolar metal complexes may still possess sufficient lipophilicity to pass through cell membranes. Additionally, ester hydrolysis might contribute to the effect observed in the MTT assay, but was not detected in the stability investigations.

Topoisomerase IIα inhibition. Several metal(II)–arene complexes have been shown to be potent inhibitors of topoisomerase IIα, an enzyme which is essential for DNA replication, transcription, and recombination, and a well-established target for cancer chemotherapy. Complexation to ruthenium(II)–arene fragments has been reported to enhance the inhibitory capacity of known topoisomerase IIα inhibitors (e.g., flavonoids[8,64]) or confer topoisomerase inhibitory capabilities to otherwise inactive free ligands (e.g., 1,3-dioxoindan-2-carboxamides,[56] 2-aryl-4-thiopyrones[65]). Consequently, the topoisomerase IIα inhibitory activity of highly cytotoxic triazole organometallics **2b** and **3b** featuring 4-methoxybenzyl residues, the less active methyl ester derivatives **2e** and **3e**, as well as their corresponding free ligands **1b** and **1e** was tested. Topoisomerase IIα inhibition is detected by decreased uncoiling of a plasmid DNA substrate from the supercoiled conformation to the relaxed conformation.

The six selected substances were incubated with the enzyme and plasmid DNA, revealing that none is able to inhibit the function of topoisomerase IIα at 25 μM or to act as a topoisomerase poison (Figure S34). Considering that the tested organometallics **2b** and **3b** show cytotoxic activity at comparable or lower concentrations in MTT assays, it is unlikely that inhibition of topoisomerase IIα contributes to their mechanism of action.

Cell cycle analysis. The cell cycle distribution of SW480 cells in response to treatment with the organometallics **2b**, **3b**, **2e**, and **3e**, and their respective free ligands **1b** and **1e** was determined at various concentrations after 48 h (Figure 6).

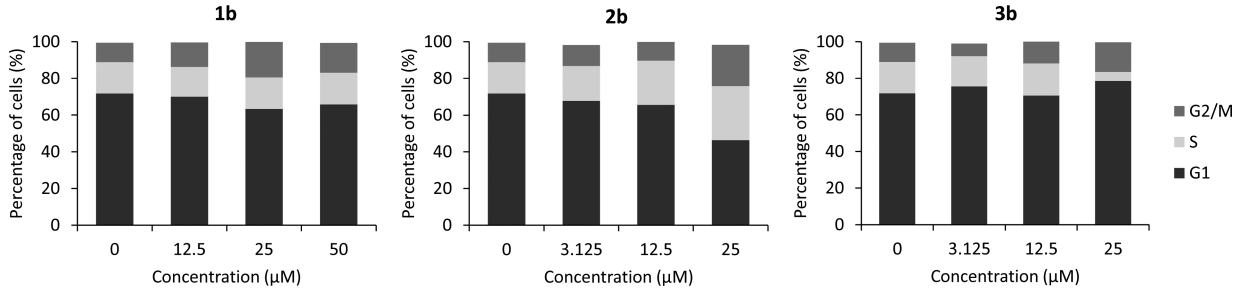

Figure 6. Cell cycle distributions (means of three independent experiments) in SW480 cells exposed to **1b** (left), **2b** (center), and **3b** (right) for 48 h compared to untreated control (0 μM) at different concentrations. Application of higher concentrations than those indicated was impossible due to limited solubility in most cases.

DOI: 10.1021/acs.inorgchem.6b02430
Inorg. Chem. XXXX, XXX, XXX–XXX

After staining with propidium iodide, the relative DNA content of the cells was determined by flow cytometry. The two ligands **1b** and **1e** show no marked effects on the cell cycle distribution at concentrations of up to 50 μM (Figure 6, Figure S35). The two ruthenium complexes **2b** and **2e** show mild effects. **2b** induces an increase of cells in the S phase at a concentration of 25 μM, whereas **2e** requires higher concentrations for comparable effects. The osmium arene complex **3b** shown to exhibit the highest antiproliferative effect almost causes an elimination of the S phase fraction (Figure 6).

In contrast, the rather inactive compound **3e** shows almost no effect on the cell cycle distribution (Figure S35). These results suggest that the cytotoxic effect of the osmium(II) derivatives is primarily exerted in the DNA synthesis (S) phase, while no definitive conclusion can be drawn from the behavior of tested ruthenium(II) compounds.

CONCLUSION

In this work, we have established the 1,2,3-triazole backbone as a promising *C,N*-ligand system for cyclometalated Ru(II) and Os(II) arene complexes. Crystal structures of all prepared organometallics were obtained and allowed the description of interesting side chain dependent crystallization behaviors. The stability and aquation of the complexes in aqueous solution containing 1% DMF, as well as anation of DMSO to replace the chlorido leaving group in the presence of 1% DMSO was described via UV−vis, ESI-MS, and NMR techniques. It could be shown that aquation is dependent on external chloride concentrations and, therefore, is considerably hindered under extracellular conditions but favored in the intracellular milieu. This behavior allows for activation of the prepared organometallics close to their biological targets.

The cytotoxicity of all organometallics and their corresponding free ligands was determined in three human cancer cell lines (A549, SW480, CH1/PA-1). While most ligands barely show any cytotoxic effect in the tested concentration range, the respective organometallics exhibit IC_{50} values down to the low micromolar range. Cytotoxicity could be correlated to cellular accumulation and seems to be mainly influenced by the lipophilicity of the ligands. The DMSO adducts of three ruthenium(II) complexes were isolated as trifalte salts and exhibited activities in a range comparable to the respective parent compounds featuring chlorido leaving groups when tested in MTT assays with the use of DMSO as solubilizer. Selected compounds were found unable to inhibit topoisomerase IIα, but the most cytotoxic compounds have a pronounced effect on cell cycle distribution, which stimulates further mode-of-action studies. The facile synthesis, modifiability, stability under physiological conditions, and high activity *in vitro* of the prepared complexes encourage future development of this promising compound class.

EXPERIMENTAL SECTION

Materials and Methods. ^{1}H, ^{13}C (APT), ^{31}P, and 2D NMR spectra were recorded on a Bruker FT-NMR spectrometer Avance III 500 MHz in deuterated dimethyl sulfoxide (DMSO-d_6) or deuterated chloroform ($CDCl_3$) and referenced to residual solvent signals[66] (^{1}H, ^{13}C) or 85% phosphoric acid (^{31}P). High resolution ESI mass spectra were recorded at the Core Facility for Mass Spectrometry of the University of Vienna (Faculty of Chemistry) on a Bruker Maxis UHR qTOF Mass Spectrometer by direct infusion. Electrospray ionization mass spectra were recorded on a Bruker AmaZon SL ion trap mass spectrometer by direct infusion. Data files were analyzed using Bruker data analysis software ESI Compass 1.3 and Data Analysis 4.0. Elemental analyses were performed at the Microanalytical Laboratory of the University of Vienna, using a PerkinElmer 2400 Series II CHNS/O Elemental Analyzer for CHN analyses and a Eurovector EA3000 Elemental Analyzer for CHNS analyses. pH values were measured with a EcoScan pH 6 pH meter equipped with a Eutech Instruments Ag/AgCl pH electrode calibrated with Alfa Aesar Specpure standard buffer solutions at pH 4.00, 7.00, and 10.00. Analytical grade solvents were purchased from commercial suppliers and used without further purification. Methanol for complexation reactions was distilled from Mg/I_2 and stored over molecular sieve (3 Å). Millipore water (Milli-Q Advantage A10, 18.2 MΩ/25 °C, 2 ppb TOC) and methanol (HPLC grade, Fisher) and were used for mass spectrometry measurements. Benzyl bromide (98%, Acros), 4-methoxybenzyl chloride (98%, Acros), 1-bromopropane (99%, Aldrich), 1-bromobutane (99%, Sigma), methyl bromoacetate (99%, Acros), sodium azide (≥99.0%, Fluka), copper(II)sulfate pentahydrate (≥99.0%, Fluka), phenylacetylene (98%, Aldrich), L-(+)-ascorbic acid sodium salt (99.0%, Fluka), silver trifluoromethanesulfonate (99+%, Acros), dimethyl sulfoxide (anal. grade, Fisher), ruthenium(III) chloride hydrate (Johnson Matthey), osmium tetroxide (Johnson Matthey), hydrazine dihydrochloride (≥98.0%, Sigma), α-terpinene (90%, Acros), sodium acetate anhydrous (≥98.5%, Fluka), molecular sieve (3 Å, beads, 4−8 mesh), phosphate buffered saline (pH 7.4, 10x, gibco), L-cysteine (Fluka), L-histidine (Merck) and L-methionine (Merck) were used without further purification.

The dimeric metal precursors dichlorido(*p*-cymene)ruthenium(II)[67] $[Ru(p\text{-cym})Cl_2]_2$ and dichlorido(*p*-cymene)osmium(II)[68] $[Os(p\text{-cym})Cl_2]_2$ were prepared according to literature procedures. Synthesis and characterization of the ligands **1a−f** can be found in the Supporting Information.

*General procedure for the synthesis of ruthenium(II) and osmium(II) arene complexes **2a−e** and **3a−e**.* Ligand **1a−f** and anhydrous sodium acetate were suspended in methanol abs. and stirred for 15 min under argon atmosphere. Subsequently, the respective metal dimer $[Ru(cym)Cl_2]_2$ or $[Os(cym)Cl_2]_2$ was added and the reaction mixture was stirred under argon atmosphere at room temperature for 16 h to 2 days, during which precipitation of the product occurred. The formed solid was filtered off, washed with cold methanol, redissolved in dichloromethane, filtered and evaporated to dryness to afford the desired organometallic complexes **2a−e** and **3a−e** in moderate to good yields.

*[Chlorido(1-benzyl-4-(2′-κC)-phenyl-(3-κN)-1,2,3-triazolato)(η^6-p-cymene)ruthenium(II)] (**2a**).* The reaction was performed according to the general complexation procedure, using **1a** (154 mg, 0.65 mmol), $[Ru(p\text{-cym})Cl_2]_2$ (200 mg, 0.33 mmol) and anhydrous sodium acetate (59 mg, 0.72 mmol) in methanol abs. (3 mL) for a reaction time of 48 h. Yield: 263 mg, 80%. ESI-HR-MS$^+$ m/z Found (Calculated): $[M-Cl]^+$ 470.1184 (470.1171), $[M+Na]^+$ 528.0767 (528.0754). Elemental Anal. Calc. for $C_{25}H_{26}ClN_3Ru$: C 59.46, H 5.19, N 8.32; Found: C 59.45, H 4.94, N 8.35. ^{1}H NMR ($CDCl_3$, 500.10 MHz, 298.2 K): δ = 8.15 (d, $^{3}J_{H,H}$ = 7 Hz, 1H, $ArH_{Ph\text{-}3'}$); 7.47 (s, 1H, $ArH_{Trz\text{-}5}$); 7.35−7.30 (m, 3H, $ArH_{Bn\text{-}3''/5''}$, $ArH_{Bn\text{-}4''}$); 7.24−7.19 (m, 3H, $ArH_{Bn\text{-}2''/6''}$, $ArH_{Ph\text{-}6'}$); 7.10 (ddd, $^{3}J_{H,H}$ = 7 Hz, 7 Hz, $^{4}J_{H,H}$ = 1 Hz, 1H, $ArH_{Ph\text{-}4'}$); 6.97 (ddd, $^{3}J_{H,H}$ = 7 Hz, 7 Hz, $^{4}J_{H,H}$ = 1 Hz, 1H, $ArH_{Ph\text{-}5'}$); 5.55 (d, $^{3}J_{H,H}$ = 6 Hz, 1H, $ArH_{Cym\text{-}c}$); 5.49 (d, $^{3}J_{H,H}$ = 6 Hz, 1H, $ArH_{Cym\text{-}d}$); 5.45 (d, $^{3}J_{H,H}$ = 6 Hz, 1H, $ArH_{Cym\text{-}d}$); 5.35 (d, $^{2}J_{H,H}$ = 15 Hz, 1H, $CH_{2,\ Bn}$); 5.22 (d, $^{3}J_{H,H}$ = 6 Hz, 1H, $ArH_{Cym\text{-}c}$); 5.18 (d, $^{2}J_{H,H}$ = 15 Hz, 1H, $CH_{2,\ Bn}$); 2.38 (sept, $^{3}J_{H,H}$ = 7 Hz, 1H, $CH_{Cym\text{-}f}$); 2.02 (s, 3H, $CH_{3,\ Cym\text{-}a}$); 0.92 (d, $^{3}J_{H,H}$ = 7 Hz, 3H, $CH_{3,\ Cym\text{-}g}$); 0.92 (d, $^{3}J_{H,H}$ = 7 Hz, 3H, $CH_{3,\ Cym\text{-}g}$); 0.84 (d, $^{3}J_{H,H}$ = 7 Hz, 3H, $CH_{3,\ Cym\text{-}g}$) ppm. ^{13}C NMR ($CDCl_3$, 125.75 MHz, 298.6 K): δ = 176.3 ($C_{Ph\text{-}2'}$); 155.5 ($C_{Trz\text{-}4}$); 139.7 ($CH_{Ph\text{-}3'}$); 135.3 ($C_{Ph\text{-}1'}$); 134.6 ($C_{Bn\text{-}1''}$); 129.1 ($CH_{Bn\text{-}3''/5''}$); 128.9 ($CH_{Bn\text{-}4''}$); 128.2 ($CH_{Bn\text{-}2''/6''}$); 127.7 ($CH_{Ph\text{-}4'}$); 122.8 ($CH_{Ph\text{-}5'}$); 122.4 ($CH_{Ph\text{-}6'}$); 117.5 ($CH_{Trz\text{-}5}$); 99.5 ($C_{Cym\text{-}e}$); 98.7 ($C_{Cym\text{-}b}$); 89.1 ($CH_{Cym\text{-}c}$); 87.3 ($CH_{Cym\text{-}d}$); 85.6 ($CH_{Cym\text{-}d}$); 83.5 ($CH_{Cym\text{-}c}$); 54.9 ($CH_{2,\ Bn}$); 30.8 ($CH_{Cym\text{-}f}$); 22.3 ($CH_{3,\ Cym\text{-}g}$); 22.2 ($CH_{3,\ Cym\text{-}g}$); 18.9 ($CH_{3,\ Cym\text{-}a}$) ppm.

*[Chlorido(1-(4″-methoxybenzyl)-4-(2′-κC)-phenyl-(3-κN)-1,2,3-triazolato)(η^6-p-cymene)ruthenium(II)] (**2b**).* The reaction was performed according to the general complexation procedure, using

DOI: 10.1021/acs.inorgchem.6b02430
Inorg. Chem. XXXX, XXX, XXX−XXX

1b (217 mg, 0.82 mmol), $[Ru(p\text{-cym})Cl_2]_2$ (250 mg, 0.41 mmol) and anhydrous sodium acetate (74 mg, 0.90 mmol) in methanol abs. (3 mL) for a reaction time of 48 h. Yield: 300 mg, 69%. ESI-HR-MS$^+$ m/z Found (Calculated): $[M-Cl]^+$ 500.1292 (500.1277), $[M+Na]^+$ 558.0874 (558.0860). Elemental Anal. Calc. for $C_{26}H_{28}ClN_3ORu$: C 58.37, H 5.27, N 7.85, S 0.00; Found: C 58.32, H 5.35, N 8.18, S < 0.02. ^{1}H NMR ($CDCl_3$, 500.10 MHz, 298.2 K): δ = 8.14 (d, $^3J_{H,H}$ = 7 Hz, 1H, $ArH_{Ph\text{-}3'}$); 7.47 (s, 1H, $ArH_{Trz\text{-}5}$); 7.22−7.18 (m, 3H, $ArH_{Ph\text{-}6'}$, $ArH_{Bn\text{-}2''/6''}$); 7.09 (ddd, $^3J_{H,H}$ = 7 Hz, 7 Hz, $^4J_{H,H}$ = 1 Hz, 1H, $ArH_{Ph\text{-}4'}$); 6.98 (ddd, $^3J_{H,H}$ = 7 Hz, 7 Hz, $^4J_{H,H}$ = 1 Hz, 1H, $ArH_{Ph\text{-}5'}$); 6.88−6.84 (m, 2H, $ArH_{Bn\text{-}3''/5''}$); 5.54 (d, $^3J_{H,H}$ = 6 Hz, 1H, $ArH_{Cym\text{-}c}$); 5.49−5.45 (m, 2H, $ArH_{Cym\text{-}d}$); 5.32 (d, $^2J_{H,H}$ = 15 Hz, 1H, $CH_{2,\ Bn}$); 5.22 (d, $^3J_{H,H}$ = 6 Hz, 1H, $ArH_{Cym\text{-}c}$); 5.15 (d, $^2J_{H,H}$ = 15 Hz, 1H, $CH_{2,\ Bn}$); 3.79 (s, 3H, $OCH_{3,\ Bn}$); 2.40 (sept, $^3J_{H,H}$ = 7 Hz, 1H, $CH_{Cym\text{-}f}$); 2.02 (s, 3H, $CH_{3,\ Cym\text{-}a}$); 0.92 (d, $^3J_{H,H}$ = 7 Hz, 3H, $CH_{3,\ Cym\text{-}g}$); 0.86−0.84 (m, 3H, $CH_{3,\ Cym\text{-}g}$) ppm. ^{13}C NMR ($CDCl_3$, 125.75 MHz, 298.6 K): δ = 176.3 ($C_{Ph\text{-}2'}$); 160.1 ($C_{Bn\text{-}4''}$); 155.4 ($C_{Trz\text{-}4}$); 139.6 ($CH_{Ph\text{-}3'}$); 135.3 ($C_{Ph\text{-}1'}$); 129.9 ($CH_{Bn\text{-}2''/6''}$); 127.7 ($CH_{Ph\text{-}4'}$); 126.4 ($C_{Bn\text{-}1''}$); 122.7 ($CH_{Ph\text{-}5'}$); 122.4 ($CH_{Ph\text{-}6'}$); 117.1 ($CH_{Trz\text{-}5}$); 114.5 ($CH_{Bn\text{-}3''/5''}$); 99.6 ($C_{Cym\text{-}e}$); 98.7 ($C_{Cym\text{-}b}$); 89.0 ($CH_{Cym\text{-}c}$); 87.4 ($CH_{Cym\text{-}d}$); 85.4 ($CH_{Cym\text{-}d}$); 83.5 ($CH_{Cym\text{-}c}$); 55.5 ($OCH_{3,\ Bn}$); 54.6 ($CH_{2,\ Bn}$); 30.8 ($CH_{Cym\text{-}f}$); 22.3 ($CH_{3,\ Cym\text{-}g}$); 22.2 ($CH_{3,\ Cym\text{-}g}$); 18.9 ($CH_{3,\ Cym\text{-}a}$) ppm.

*[Chlorido(1-propyl-4-(2′-κC)-phenyl-(3-κN)-1,2,3-triazolato)(η^6-p-cymene)ruthenium(II)] (**2c**).* The reaction was performed according to the general complexation procedure, using **1c** (153 mg, 0.82 mmol), $[Ru(p\text{-cym})Cl_2]_2$ (250 mg, 0.41 mmol) and anhydrous sodium acetate (74 mg, 0.90 mmol) in methanol abs. (3 mL) for a reaction time of 48 h. Yield: 213 mg, 57%. ESI-HR-MS$^+$ m/z Found (Calculated): $[M-Cl]^+$ 422.1176 (422.1170), $[M+Na]^+$ 480.0758 (480.0753). Elemental Anal. Calc. for $C_{21}H_{26}ClN_3Ru \cdot 0.75H_2O$: C 53.61, H 5.89, N 8.93; Found: C 53.67, H 5.65, N 8.99. ^{1}H NMR ($CDCl_3$, 500.32 MHz, 300.5 K): δ = 8.15 (d, $^3J_{H,H}$ = 7 Hz, 1H, $ArH_{Ph\text{-}3'}$); 7.55 (s, 1H, $ArH_{Trz\text{-}5}$); 7.24 (d, $^3J_{H,H}$ = 7 Hz, 1H, $ArH_{Ph\text{-}6'}$); 7.10 (dd, $^3J_{H,H}$ = 7 Hz, 7 Hz, 1H, $ArH_{Ph\text{-}4'}$); 6.97 (dd, $^3J_{H,H}$ = 7 Hz, 7 Hz, 1H, $ArH_{Ph\text{-}5'}$); 5.54 (d, $^3J_{H,H}$ = 6 Hz, 1H, $ArH_{Cym\text{-}c}$); 5.49 (d, $^3J_{H,H}$ = 6 Hz, 1H, $ArH_{Cym\text{-}d}$); 5.45 (d, $^3J_{H,H}$ = 6 Hz, 1H, $ArH_{Cym\text{-}d}$); 5.20 (d, $^3J_{H,H}$ = 6 Hz, 1H, $ArH_{Cym\text{-}c}$); 4.27−4.20 (m, 1H, $CH_{2,\ Prop\text{-}1''}$); 4.11−4.03 (m, 1H, $CH_{2,\ Prop\text{-}1''}$); 2.42 (sept, $^3J_{H,H}$ = 7 Hz, 1H, $CH_{Cym\text{-}f}$); 2.03 (s, 3H, $CH_{3,\ Cym\text{-}a}$); 1.94−1.83 (m, 2H, $CH_{2,\ Prop\text{-}2''}$); 0.95−0.88 (m, 9H, $CH_{3,\ Prop\text{-}3''}$, $CH_{3,\ Cym\text{-}g}$) ppm. ^{13}C NMR ($CDCl_3$, 125.81 MHz, 300.6 K): δ = 176.2 ($C_{Ph\text{-}2'}$); 155.2 ($C_{Trz\text{-}4}$); 139.6 ($CH_{Ph\text{-}3'}$); 135.4 ($C_{Ph\text{-}1'}$); 127.7 ($CH_{Ph\text{-}4'}$); 122.7 ($CH_{Ph\text{-}5'}$); 122.3 ($CH_{Ph\text{-}6'}$); 117.2 ($CH_{Trz\text{-}5}$); 99.4 ($C_{Cym\text{-}e}$); 99.0 ($C_{Cym\text{-}b}$); 88.8 ($CH_{Cym\text{-}c}$); 87.8 ($CH_{Cym\text{-}d}$); 85.2 ($CH_{Cym\text{-}d}$); 83.3 ($CH_{Cym\text{-}c}$); 53.1 ($CH_{2,\ Prop\text{-}1''}$); 30.9 ($CH_{Cym\text{-}f}$); 23.6 ($CH_{2,\ Prop\text{-}2''}$); 22.4 ($CH_{3,\ Cym\text{-}g}$); 22.1 ($CH_{3,\ Cym\text{-}g}$); 18.9 ($CH_{3,\ Cym\text{-}a}$); 11.0 ($CH_{3,\ Prop\text{-}3''}$) ppm.

*[Chlorido(1-butyl-4-(2′-κC)-phenyl-(3-κN)-1,2,3-triazolato)(η^6-p-cymene)ruthenium(II)] (**2d**).* The reaction was performed according to the general complexation procedure, using **1d** (132 mg, 0.65 mmol), $[Ru(p\text{-cym})Cl_2]_2$ (200 mg, 0.33 mmol) and anhydrous sodium acetate (59 mg, 0.72 mmol) in methanol abs. (3 mL) for a reaction time of 48 h. Yield: 250 mg, 81%. ESI-HR-MS$^+$ m/z Found (Calculated): $[M-Cl]^+$ 436.1326 (436.1327), $[M+Na]^+$ 494.0905 (494.0910). Elemental Anal. Calc. for $C_{22}H_{28}ClN_3Ru \cdot 0.5H_2O$: C 55.05, H 6.09, N 8.75, S 0.00; Found: C 54.94, H 5.85, N 8.54, S < 0.02. ^{1}H NMR ($CDCl_3$, 500.32 MHz, 299:8 K): δ = 8.14 (d, $^3J_{H,H}$ = 7 Hz, 1H, $ArH_{Ph\text{-}3'}$); 7.55 (s, 1H, $ArH_{Trz\text{-}5}$); 7.22 (d, $^3J_{H,H}$ = 7 Hz, 1H, $ArH_{Ph\text{-}6'}$); 7.09 (dd, $^3J_{H,H}$ = 7 Hz, 7 Hz, 1H, $ArH_{Ph\text{-}4'}$); 6.97 (dd, $^3J_{H,H}$ = 7 Hz, 7 Hz, 1H, $ArH_{Ph\text{-}5'}$); 5.53 (d, $^3J_{H,H}$ = 6 Hz, 1H, $ArH_{Cym\text{-}c}$); 5.48 (d, $^3J_{H,H}$ = 6 Hz, 1H, $ArH_{Cym\text{-}d}$); 5.45 (d, $^3J_{H,H}$ = 6 Hz, 1H, $ArH_{Cym\text{-}d}$); 5.20 (d, $^3J_{H,H}$ = 6 Hz, 1H, $ArH_{Cym\text{-}c}$); 4.26−4.19 (m, 1H, $CH_{2,\ But\text{-}1''}$); 4.08−4.01 (m, 1H, $CH_{2,\ But\text{-}1''}$); 2.41 (sept, $^3J_{H,H}$ = 7 Hz, 1H, $CH_{Cym\text{-}f}$); 2.02 (s, 3H, $CH_{3,\ Cym\text{-}a}$); 1.83−1.78 (m, 2H, $CH_{2,\ But\text{-}2''}$); 1.34−1.21 (m, 2H, $CH_{2,\ But\text{-}3''}$); 0.96−0.87 (m, 9H, $CH_{3,\ But\text{-}4''}$, $CH_{3,\ Cym\text{-}g}$) ppm. ^{13}C NMR ($CDCl_3$, 125.81 MHz, 301.0K): δ = 176.2 ($C_{Ph\text{-}2'}$); 155.2 ($C_{Trz\text{-}4}$); 139.6 ($CH_{Ph\text{-}3'}$); 135.4 ($C_{Ph\text{-}1'}$); 127.6 ($CH_{Ph\text{-}4'}$); 122.7 ($CH_{Ph\text{-}5'}$); 122.3 ($CH_{Ph\text{-}6'}$); 117.3 ($CH_{Trz\text{-}5}$); 99.4 ($C_{Cym\text{-}e}$); 99.0 ($C_{Cym\text{-}b}$); 88.8 ($CH_{Cym\text{-}c}$); 87.7 ($CH_{Cym\text{-}d}$); 85.3 ($CH_{Cym\text{-}d}$); 83.3 ($CH_{Cym\text{-}c}$); 51.2 ($CH_{2,\ But\text{-}1''}$); 32.1 ($CH_{2,\ But\text{-}2''}$); 30.9 ($CH_{Cym\text{-}f}$); 22.4 ($CH_{3,\ Cym\text{-}g}$); 22.1 ($CH_{3,\ Cym\text{-}g}$); 19.7 ($CH_{2,\ But\text{-}3''}$); 18.8 ($CH_{3,\ Cym\text{-}a}$); 13.5 ($CH_{3,\ But\text{-}4''}$) ppm.

*[Chlorido(methyl-2″-(4-(2′-κC)-phenyl-(3-κN)-1,2,3-triazol-1-ylato)acetato)(η^6-p-cymene)ruthenium(II)] (**2e**).* The reaction was performed according to the general complexation procedure, using **1e** (177 mg, 0.82 mmol), $[Ru(p\text{-cym})Cl_2]_2$ (250 mg, 0.41 mmol) and anhydrous sodium acetate (74 mg, 0.90 mmol) in methanol abs. (3 mL) for a reaction time of 48 h. Yield: 243 mg, 61%. ESI-HR-MS$^+$ m/z Found (Calculated): $[M-Cl]^+$ 452.0914 (452.0912), $[M+Na]^+$ 510.0494 (510.0495). Elemental Anal. Calc. for $C_{21}H_{24}ClN_3O_2Ru \cdot 0.5H_2O$: C 50.86, H 5.08, N 8.47, S 0.00; Found: C 51.04, H 4.94, N 8.55, S < 0.02. ^{1}H NMR ($CDCl_3$, 500.10 MHz, 299.9 K): δ = 8.16 (d, $^3J_{H,H}$ = 7 Hz, 1H, $ArH_{Ph\text{-}3'}$); 7.74 (s, 1H, $ArH_{Trz\text{-}5}$); 7.17 (dd, $^3J_{H,H}$ = 7 Hz, $^4J_{H,H}$ = 1 Hz, 1H, $ArH_{Ph\text{-}6'}$); 7.14 (ddd, $^3J_{H,H}$ = 7 Hz, 7 Hz, $^4J_{H,H}$ = 1 Hz, 1H, $ArH_{Ph\text{-}4'}$); 7.01 (ddd, $^3J_{H,H}$ = 7 Hz, 7 Hz, $^4J_{H,H}$ = 1 Hz, 1H, $ArH_{Ph\text{-}5'}$); 5.51 (d, $^3J_{H,H}$ = 6 Hz, 1H, $ArH_{Cym\text{-}c}$); 5.47 (d, $^3J_{H,H}$ = 6 Hz, 1H, $ArH_{Cym\text{-}d}$); 5.44 (d, $^3J_{H,H}$ = 6 Hz, 1H, $ArH_{Cym\text{-}d}$); 5.20 (d, $^3J_{H,H}$ = 6 Hz, 1H, $ArH_{Cym\text{-}c}$); 4.61 (d, $^2J_{H,H}$ = 18 Hz, 1H, $CH_{2,\ Ac}$); 4.53 (d, $^2J_{H,H}$ = 18 Hz, 1H, $CH_{2,\ Ac}$); 3.67 (s, 3H, $OCH_{3,\ Ac}$); 2.35 (sept, $^3J_{H,H}$ = 7 Hz, 1H, $CH_{Cym\text{-}f}$); 1.98 (s, 3H, $CH_{3,\ Cym\text{-}a}$); 0.91 (d, $^3J_{H,H}$ = 7 Hz, 3H, $CH_{3,\ Cym\text{-}g}$); 0.87 (d, $^3J_{H,H}$ = 7 Hz, 3H, $CH_{3,\ Cym\text{-}g}$) ppm. ^{13}C NMR ($CDCl_3$, 125.75 MHz, 300.4 K): δ = 176.2 ($C_{Ph\text{-}2'}$); 166.9 (CO_{Ac}); 154.9 ($C_{Trz\text{-}4}$); 139.9 ($CH_{Ph\text{-}3'}$); 135.3 ($C_{Ph\text{-}1'}$); 127.7 ($CH_{Ph\text{-}4'}$); 122.9 ($CH_{Ph\text{-}5'}$); 122.4 ($CH_{Ph\text{-}6'}$); 119.8 ($CH_{Trz\text{-}5}$); 99.5 ($C_{Cym\text{-}e}$); 99.1 ($C_{Cym\text{-}b}$); 88.9 ($CH_{Cym\text{-}c}$); 88.0 ($CH_{Cym\text{-}d}$); 85.5 ($CH_{Cym\text{-}d}$); 83.3 ($CH_{Cym\text{-}c}$); 52.9 ($OCH_{3,\ Ac}$); 50.9 ($CH_{2,\ Ac}$); 30.8 ($CH_{Cym\text{-}f}$); 22.3 ($CH_{3,\ Cym\text{-}g}$); 22.1 ($CH_{3,\ Cym\text{-}g}$); 18.7 ($CH_{3,\ Cym\text{-}a}$) ppm.

*[Chlorido(1-benzyl-4-(2′-κC)-phenyl-(3-κN)-1,2,3-triazolato)(η^6-p-cymene)osmium(II)] (**3a**).* The reaction was performed according to the general complexation procedure, using **1a** (119 mg, 0.51 mmol), $[Os(p\text{-cym})Cl_2]_2$ (200 mg, 0.25 mmol) and anhydrous sodium acetate (46 mg, 0.56 mmol) in methanol abs. (5 mL) for a reaction time of 48 h. Yield: 192 mg, 64%. ESI-HR-MS$^+$ m/z Found (Calculated): $[M-Cl]^+$ 560.1748 (560.1737), $[M+Na]^+$ 618.1325 (618.1312), $[2M+Na]^+$ 1211.2710 (1211.2710). Elemental Anal. Calc. for $C_{25}H_{26}ClN_3Os$: C 50.54, H 4.41, N 7.07, S 0.00; Found: C 50.45, H 4.48, N 6.81, S < 0.02. ^{1}H NMR ($CDCl_3$, 500.10 MHz, 298.2 K): δ = 8.01 (d, $^3J_{H,H}$ = 7 Hz, 1H, $ArH_{Ph\text{-}3'}$); 7.46 (s, 1H, $ArH_{Trz\text{-}5}$); 7.41−7.37. (m, 3H, $ArH_{Bn\text{-}3''/5''}$, $ArH_{Bn\text{-}4''}$); 7.32 (dd, $^3J_{H,H}$ = 7 Hz, $^4J_{H,H}$ = 1 Hz, 1H, $ArH_{Ph\text{-}6'}$); 7.30−7.24 (m, 2H, $ArH_{Bn\text{-}2''/6''}$); 7.05 (ddd, $^3J_{H,H}$ = 7 Hz, 7 Hz, $^4J_{H,H}$ = 1 Hz, 1H, $ArH_{Ph\text{-}4'}$); 6.94 (ddd, $^3J_{H,H}$ = 7 Hz, 7 Hz, $^4J_{H,H}$ = 1 Hz, 1H, $ArH_{Ph\text{-}5'}$); 5.65−5.59 (m, 2H, $ArH_{Cym\text{-}d}$, $CH_{2,\ Bn}$); 5.55−5.52 (m, 2H, $ArH_{Cym\text{-}c}$, $ArH_{Cym\text{-}d}$); 5.47 (d, $^2J_{H,H}$ = 15 Hz, $CH_{2,\ Bn}$); 5.35 (d, $^3J_{H,H}$ = 5 Hz, 1H, $ArH_{Cym\text{-}c}$); 2.39 (sept, $^3J_{H,H}$ = 7 Hz, 1H, $CH_{Cym\text{-}f}$); 2.18 (s, 3H, $CH_{3,\ Cym\text{-}a}$); 0.96−0.90 (m, 6H, $CH_{3,\ Cym\text{-}g}$) ppm. ^{13}C NMR ($CDCl_3$, 125.75 MHz, 299.3 K): δ = 162.6 ($C_{Ph\text{-}2'}$); 157.4 ($C_{Trz\text{-}4}$); 139.5 ($CH_{Ph\text{-}3'}$); 136.1 ($C_{Ph\text{-}1'}$); 134.5 ($C_{Bn\text{-}1''}$); 128.2 ($CH_{Bn\text{-}3''/5''}$); 128.9 ($CH_{Bn\text{-}4''}$); 128.4 ($CH_{Ph\text{-}4'}$); 128.2 ($CH_{Bn\text{-}2''/6''}$); 122.7 ($CH_{Ph\text{-}5'}$); 122.1 ($CH_{Ph\text{-}6'}$); 117.7 ($CH_{Trz\text{-}5}$); 91.7 ($C_{Cym\text{-}b}$); 90.3 ($C_{Cym\text{-}e}$); 79.3 ($CH_{Cym\text{-}c}$); 78.2 ($CH_{Cym\text{-}d}$); 76.6 ($CH_{Cym\text{-}d}$); 73.3 ($CH_{Cym\text{-}c}$); 55.0 ($CH_{2,\ Bn}$); 31.1 ($CH_{Cym\text{-}f}$); 22.5 ($CH_{3,\ Cym\text{-}g}$); 22.7 ($CH_{3,\ Cym\text{-}g}$); 18.7 ($CH_{3,\ Cym\text{-}a}$) ppm.

*[Chlorido(1-(4″-methoxybenzyl)-4-(2′-κC)-phenyl-(3-κN)-1,2,3-triazolato)(η^6-p-cymene)osmium(II)] (**3b**).* The reaction was performed according to the general complexation procedure, using **1b** (134 mg, 0.51 mmol), $[Os(p\text{-cym})Cl_2]_2$ (200 mg, 0.25 mmol) and anhydrous sodium acetate (46 mg, 0.56 mmol) in methanol abs. (3 mL) for a reaction time of 48 h. Yield: 248 mg, 78%. ESI-HR-MS$^+$ m/z Found (Calculated): $[M-Cl]^+$ 590.1856 (590.1843), $[M+Na]^+$ 648.1432 (648.1418), $[2M+Na]^+$ 1271.2969 (1271.2922). Elemental Anal. Calc. for $C_{26}H_{28}ClN_3OOs$: C 50.03, H 4.52, N 6.73, S 0.00; Found: C 49.89, H 4.61, N 6.52, S < 0.02. ^{1}H NMR ($CDCl_3$, 500.10 MHz, 297.3 K): δ = 8.01 (d, $^3J_{H,H}$ = 7 Hz, 1H, $ArH_{Ph\text{-}3'}$); 7.46 (s, 1H, $ArH_{Trz\text{-}5}$); 7.28 (dd, $^3J_{H,H}$ = 7 Hz, $^4J_{H,H}$ = 1 Hz, 1H, $ArH_{Ph\text{-}6'}$); 7.24−7.20 (m, 2H, $ArH_{Bn\text{-}2''/6''}$); 7.04 (ddd, $^3J_{H,H}$ = 7 Hz, 7 Hz, $^4J_{H,H}$ = 1 Hz, 1H, $ArH_{Ph\text{-}4'}$); 6.94 (ddd, $^3J_{H,H}$ = 7 Hz, 7 Hz, $^4J_{H,H}$ = 1 Hz, 1H, $ArH_{Ph\text{-}5'}$); 6.90−6.87 (m, 2H, $ArH_{Bn\text{-}3''/5''}$); 5.63 (d, $^3J_{H,H}$ = 5 Hz, 1H, $ArH_{Cym\text{-}d}$); 5.53−5.50 (m, 2H, $ArH_{Cym\text{-}c}$, $ArH_{Cym\text{-}d}$); 5.42 (d, $^2J_{H,H}$ = 15 Hz, 1H, $CH_{2,\ Bn}$); 5.37 (d, $^3J_{H,H}$ = 5 Hz, 1H, $ArH_{Cym\text{-}c}$); 5.28 (d, $^2J_{H,H}$ = 15 Hz, 1H, $CH_{2,\ Bn}$); 3.80 (s, 3H, $OCH_{3,\ Bn}$); 2.37 (sept, $^3J_{H,H}$ = 7 Hz,

DOI: 10.1021/acs.inorgchem.6b02430
Inorg. Chem. XXXX, XXX, XXX−XXX

1H, $CH_{Cym\text{-}f}$); 2.17 (s, 3H, $CH_{3,\ Cym\text{-}a}$); 0.94−0.88 (m, 6H, $CH_{3,\ Cym\text{-}g}$) ppm. ^{13}C NMR ($CDCl_3$, 125.75 MHz, 299.3 K): δ = 162.6 ($C_{Ph\text{-}2'}$); 160.2 ($C_{Bn\text{-}4''}$); 157.5 ($C_{Trz\text{-}4}$); 139.5 ($C_{Ph\text{-}3'}$); 136.1 ($C_{Ph\text{-}1'}$); 129.9 ($CH_{Bn\text{-}2''/6''}$); 128.5 ($CH_{Ph\text{-}4'}$); 126.0 ($C_{Bn\text{-}1''}$); 122.7 ($CH_{Ph\text{-}5'}$); 122.0 ($CH_{Ph\text{-}6'}$); 117.1 ($CH_{Trz\text{-}5}$); 114.7 ($CH_{Bn\text{-}3''/5''}$); 91.8 ($C_{Cym\text{-}b}$); 90.4 ($C_{Cym\text{-}e}$); 79.2 ($CH_{Cym\text{-}c}$); 78.3 ($CH_{Cym\text{-}d}$); 76.3 ($CH_{Cym\text{-}d}$); 73.2 ($CH_{Cym\text{-}c}$); 55.5 ($OCH_{3,\ Bn}$); 54.8 ($CH_{2,\ Bn}$); 31.1 ($CH_{Cym\text{-}f}$); 22.7 ($CH_{3,\ Cym\text{-}g}$); 22.5 ($CH_{3,\ Cym\text{-}g}$); 18.7 ($CH_{3,\ Cym\text{-}a}$) ppm.

*[Chlorido(1-propyl-4-(2′-κC)-phenyl-(3-κN)-1,2,3-triazolato)(η⁶-p-cymene)osmium(II)] (**3c**).* The reaction was performed according to the general complexation procedure, using **1c** (95 mg, 0.51 mmol), $[Os(p\text{-cym})Cl_2]_2$ (200 mg, 0.25 mmol) and anhydrous sodium acetate (46 mg, 0.56 mmol) in methanol abs. (3 mL) for a reaction time of 48 h. Yield: 196 mg, 71%. ESI-HR-MS^+ *m/z* Found (Calculated): $[M-Cl]^+$ 512.1748 (512.1737), $[M+Na]^+$ 570.1323 (570.1312), $[2M+Na]^+$ 1115.2728 (1115.2708). Elemental Anal. Calc. for $C_{21}H_{26}ClN_3Os$: C 46.18, H 4.80, N 7.69, S 0.00; Found: C 45.91, H 4.88, N 7.35, S < 0.02. ^1H NMR ($CDCl_3$, 500.10 MHz, 297.8 K): δ = 8.01 (d, $^3J_{H,H}$ = 7 Hz, 1H, $ArH_{Ph\text{-}3'}$); 7.58 (s, 1H, $ArH_{Trz\text{-}5}$); 7.31 (d, $^3J_{H,H}$ = 7 Hz, 1H, $ArH_{Ph\text{-}6'}$); 7.05 (dd, $^3J_{H,H}$ = 7 Hz, 7 Hz, 1H, $ArH_{Ph\text{-}4'}$); 6.95 (dd, $^3J_{H,H}$ = 7 Hz, 7 Hz, 1H, $ArH_{Ph\text{-}5'}$); 5.61 (d, $^3J_{H,H}$ = 5 Hz, 1H, $ArH_{Cym\text{-}c}$); 5.54−5.50 (m, 2H, $ArH_{Cym\text{-}c}$, $ArH_{Cym\text{-}d}$); 5.36 (d, $^3J_{H,H}$ = 5 Hz, 1H, $ArH_{Cym\text{-}c}$); 4.27−4.20 (m, 1H, $CH_{2,\ Prop\text{-}1''}$); 4.11−4.04 (m, 1H, $CH_{2,\ Prop\text{-}1''}$); 2.37 (sept, $^3J_{H,H}$ = 7 Hz, 1H, $CH_{Cym\text{-}f}$); 2.17 (s, 3H, $CH_{3,\ Cym\text{-}a}$); 1.94−1.82 (m, 2H, $CH_{2,\ Prop\text{-}2''}$); 0.94−0.88 (m, 9H, $CH_{3,\ Prop\text{-}3''}$, $CH_{3,\ Cym\text{-}g}$) ppm. ^{13}C NMR ($CDCl_3$, 125.75 MHz, 299.0 K): δ = 162.5 ($C_{Ph\text{-}2'}$); 157.1 ($C_{Trz\text{-}4}$); 139.4 ($CH_{Ph\text{-}3'}$); 136.2 ($C_{Ph\text{-}1'}$); 128.3 ($CH_{Ph\text{-}4'}$); 122.7 ($CH_{Ph\text{-}5'}$); 122.0 ($CH_{Ph\text{-}6'}$); 117.5 ($CH_{Trz\text{-}5}$); 92.0 ($C_{Cym\text{-}b}$); 90.1 ($C_{Cym\text{-}e}$); 78.9 ($CH_{Cym\text{-}c}$); 78.5 ($CH_{Cym\text{-}d}$); 76.2 ($CH_{Cym\text{-}d}$); 73.0 ($CH_{Cym\text{-}c}$); 53.1 ($CH_{2,\ Prop\text{-}1''}$); 31.1 ($CH_{Cym\text{-}f}$); 23.6 ($CH_{2,\ Prop\text{-}2''}$); 22.8 ($CH_{3,\ Cym\text{-}g}$); 22.4 ($CH_{3,\ Cym\text{-}g}$); 18.7 ($CH_{3,\ Cym\text{-}a}$); 11.0 ($CH_{3,\ Prop\text{-}3''}$) ppm.

*[Chlorido(1-butyl-4-(2′-κC)-phenyl-(3-κN)-1,2,3-triazolato)(η⁶-p-cymene)osmium(II)] (**3d**).* The reaction was performed according to the general complexation procedure, using **1d** (102 mg, 0.51 mmol), $[Os(p\text{-cym})Cl_2]_2$ (200 mg, 0.25 mmol) and anhydrous sodium acetate (46 mg, 0.56 mmol) in methanol abs. (5 mL) for a reaction time of 48 h. Yield: 222 mg, 78%. ESI-HR-MS^+ *m/z* Found (Calculated): $[M-Cl]^+$ 526.1891 (526.1893), $[M+Na]^+$ 584.1473 (584.1469), $[2M+Na]^+$ 1143.3113 (1143.3022). Elemental Anal. Calc. for $C_{22}H_{28}ClN_3Os \cdot 0.5H_2O$: C 46.42, H 5.14, N 7.38; Found: C 46.44, H 5.04, N 7.31. ^1H NMR ($CDCl_3$, 500.10 MHz, 298.2 K): δ = 8.01 (d, $^3J_{H,H}$ = 7 Hz, 1H, $ArH_{Ph\text{-}3'}$); 7.58 (s, 1H, $ArH_{Trz\text{-}5}$); 7.31 (dd; $^3J_{H,H}$ = 7 Hz, $^4J_{H,H}$ = 1 Hz, 1H, $ArH_{Ph\text{-}6'}$); 7.05 (ddd, $^3J_{H,H}$ = 7 Hz, 7 Hz, $^4J_{H,H}$ = 1 Hz, 1H, $ArH_{Ph\text{-}4'}$); 6.95 (ddd, $^3J_{H,H}$ = 7 Hz, 7 Hz, $^4J_{H,H}$ = 1 Hz, 1H, $ArH_{Ph\text{-}5'}$); 5.61 (d, $^3J_{H,H}$ = 5 Hz, 1H, $ArH_{Cym\text{-}d}$); 5.53−5.49 (m, 2H, $ArH_{Cym\text{-}c}$, $ArH_{Cym\text{-}d}$); 5.36 (d, $^3J_{H,H}$ = 5 Hz, 1H, $ArH_{Cym\text{-}c}$); 4.33−4.26 (m, 1H, $CH_{2,\ But\text{-}1''}$); 4.17−4.10 (m, 1H, $CH_{2,\ But\text{-}1''}$); 2.37 (sept, $^3J_{H,H}$ = 7 Hz, 1H, $CH_{Cym\text{-}f}$); 2.16 (s, 3H, $CH_{3,\ Cym\text{-}a}$); 1.85 (tt, $^3J_{H,H}$ = 7 Hz, 7 Hz, 2H, $CH_{2,\ But\text{-}2''}$); 1.36−1.25 (m, 2H, $CH_{2,\ But\text{-}3''}$); 0.96−0.91 (m, 9H, $CH_{3,\ But\text{-}4''}$, $CH_{3,\ Cym\text{-}g}$) ppm. ^{13}C NMR ($CDCl_3$, 125.75 MHz, 298.2 K): δ = 162.5 ($C_{Ph\text{-}2'}$); 157.1 ($C_{Trz\text{-}4}$); 139.4 ($CH_{Ph\text{-}3'}$); 136.2 ($C_{Ph\text{-}1'}$); 128.4 ($CH_{Ph\text{-}4'}$); 122.7 ($CH_{Ph\text{-}5'}$); 122.0 ($CH_{Ph\text{-}6'}$); 117.4 ($CH_{Trz\text{-}5}$); 91.9 ($C_{Cym\text{-}b}$); 90.1 ($C_{Cym\text{-}e}$); 78.9 ($CH_{Cym\text{-}c}$); 78.5 ($CH_{Cym\text{-}d}$); 76.3 ($CH_{Cym\text{-}d}$); 73.1 ($CH_{Cym\text{-}c}$); 51.3 ($CH_{2,\ But\text{-}1''}$); 32.1 ($CH_{2,\ But\text{-}2''}$); 31.1 ($CH_{Cym\text{-}f}$); 22.8 ($CH_{3,\ Cym\text{-}g}$); 22.4 ($CH_{3,\ Cym\text{-}g}$); 19.7 ($CH_{2,\ But\text{-}3''}$); 18.7 ($CH_{3,\ Cym\text{-}a}$); 13.5 ($CH_{3,\ But\text{-}4''}$) ppm.

*[Chlorido(methyl-2″-(4-(2′-κC)-phenyl-(3-κN)-1,2,3-triazol-1-ylato)acetato)(η⁶-p-cymene) osmium(II)] (**3e**).* The reaction was performed according to the general complexation procedure, using **1e** (110 mg, 0.51 mmol), $[Os(p\text{-cym})Cl_2]_2$ (200 mg, 0.25 mmol) and anhydrous sodium acetate (46 mg, 0.56 mmol) in methanol abs. (3 mL) for a reaction time of 48 h. Yield: 152 mg, 52%. ESI-HR-MS^+ *m/z* Found (Calculated): $[M-Cl]^+$ 542.1494 (542.1478), $[M+Na]^+$ 600.1069 (600.1054), $[2M+Na]^+$ 1175.2267 (1175.2192). Elemental Anal. Calc. for $C_{21}H_{24}ClN_3O_2Os$: C 43.78, H 4.20, N 7.29, S 0.00, Found: C 43.80, H 4.28, N 7.06, S < 0.02. ^1H NMR ($CDCl_3$, 500.10 MHz, 297.2K): δ = 8.03 (d, $^3J_{H,H}$ = 7 Hz, 1H, $ArH_{Ph\text{-}3'}$); 7.79 (s, 1H, $ArH_{Trz\text{-}5}$); 7.23 (d, $^3J_{H,H}$ = 7 Hz, 1H, $ArH_{Ph\text{-}6'}$); 7.09 (dd, $^3J_{H,H}$ = 7 Hz, 7 Hz, 1H, $ArH_{Ph\text{-}4'}$); 6.98 (dd, $^3J_{H,H}$ = 7 Hz, 7 Hz, 1H, $ArH_{Ph\text{-}5'}$); 5.60 (d, $^3J_{H,H}$ = 5 Hz, 1H, $ArH_{Cym\text{-}d}$); 5.51−5.48 (m, 2H, $ArH_{Cym\text{-}c}$, $ArH_{Cym\text{-}d}$); 5.36 (d, $^3J_{H,H}$ = 5 Hz, 1H, $ArH_{Cym\text{-}c}$); 4.67 (d, $^2J_{H,H}$ = 18 Hz, 1H, $CH_{2,\ Ac}$); 4.52 (d, $^2J_{H,H}$ = 18 Hz, 1H, $CH_{2,\ Ac}$); 3.68 (s, 3H, $OCH_{3,\ Ac}$); 2.30 (sept, $^3J_{H,H}$ = 7 Hz, 1H, $CH_{Cym\text{-}f}$); 2.14 (s, 3H, $CH_{3,\ Cym\text{-}a}$); 0.91−0.87 (m, 6H, $CH_{3,\ Cym\text{-}g}$) ppm. ^{13}C NMR ($CDCl_3$, 125.75 MHz, 299.1 K): δ = 166.8 (CO_{Ac}); 162.5 ($C_{Ph\text{-}2'}$); 156.8 ($C_{Trz\text{-}4}$); 139.7 ($CH_{Ph\text{-}3'}$); 136.1 ($C_{Ph\text{-}1'}$); 128.4 ($CH_{Ph\text{-}4'}$); 122.9 ($CH_{Ph\text{-}5'}$); 122.1 ($CH_{Ph\text{-}6'}$); 120.2 ($CH_{Trz\text{-}5}$); 92.3 ($C_{Cym\text{-}b}$); 90.2 ($C_{Cym\text{-}e}$); 79.1 ($CH_{Cym\text{-}c}$); 78.7 ($CH_{Cym\text{-}d}$); 76.6 ($CH_{Cym\text{-}d}$); 73.0 ($CH_{Cym\text{-}c}$); 52.9 ($OCH_{3,\ Ac}$); 51.0 ($CH_{2,\ Ac}$); 31.0 ($CH_{Cym\text{-}f}$); 22.7 ($CH_{3,\ Cym\text{-}g}$); 22.3 ($CH_{3,\ Cym\text{-}g}$); 18.6 ($CH_{3,\ Cym\text{-}a}$) ppm.

*General procedure for the synthesis of DMSO adducts **2a′**, **2e′**, **3e′**.* The respective chlorido metal complex (1.0 equiv) and DMSO (2.0 equiv) were suspended in THF (10 mL). Silver trifluoromethanesulfonate (2.0 equiv) was added, after which the reaction mixture was stirred for 30 min in darkness at room temperature. The solvent was evaporated *in vacuo*, the residue redissolved in DCM, filtered, diluted with DCM to a volume of 20 mL and washed three times with $H_2O_{tridest.}$ (10 mL). The organic layer was separated, evaporated to dryness, purified by flash chromatography on silica (0 to 5% MeOH in DCM) and dried *in vacuo* to afford the desired products as pale yellow solids.

*[(κS-Dimethyl sulfoxide)(1-benzyl-4-(2′-κC)-phenyl-1,2,3-(3-κN)-triazolato)(η⁶-p-cymene)ruthenium(II)] trifluoromethanesulfonate (**2a′**).* The reaction was performed according to the general leaving group exchange procedure, using **2a** (150 mg, 0.30 mmol), DMSO (42 μL, 0.60 mmol, 2.0 equiv) and AgOTf (153 mg, 0.60 mmol). Yield: 158 mg, 76%. ESI-HR-MS^+ *m/z* Found (Calculated): $[M-DMSO]^+$ 470.1175 (470.1171), $[M]^+$ 548.1316 (548.1311). Elemental Anal. Calc. for $C_{28}H_{32}F_3N_3O_4RuS_2$: C 48.27, H 4.63, N 6.03, S: 9.18; Found: C 48.14, H 4.63, N 6.02, S 9.12. ^1H NMR ($CDCl_3$, 500.10 MHz, 298.2 K): δ = 8.28 (s, 1H, $ArH_{Trz\text{-}5}$); 7.91 (d, $^3J_{H,H}$ = 7 Hz, 1H, $ArH_{Ph\text{-}3'}$); 7.51−7.45 (m, 3H, $ArH_{Ph\text{-}6'}$, $ArH_{Bn\text{-}2''/6''}$); 7.42−7.34 (m, 3H, $ArH_{Bn\text{-}3''/5''}$, $ArH_{Bn\text{-}4''}$); 7.18 (ddd, $^3J_{H,H}$ = 7 Hz, 7 Hz, $^4J_{H,H}$ = 2 Hz, 1H, $ArH_{Ph\text{-}4'}$); 7.14 (ddd, $^3J_{H,H}$ = 7 Hz, 7 Hz, $^4J_{H,H}$ = 1 Hz); 4.01−5.97 (m, 1H, ArHCym-c); 5.83−5.79 (m, 2H, $ArH_{Cym\text{-}d}$); 5.78−5.70 (m, 2H, $CH_{2,\ Bn}$); 5.63−5.59 (m, 1H, $ArH_{Cym\text{-}c}$); 2.62 (sept, $^3J_{H,H}$ = 7 Hz, 1H, $ArH_{Cym\text{-}f}$); 2.62 (s, 3H, $CH_{3,\ DMSO}$); 2.39 (s, 3H, $CH_{3,\ DMSO}$); 2.23 (s, 3H, $CH_{3,\ Cym\text{-}a}$); 1.00 (d, $^3J_{H,H}$ = 7 Hz, 3H, $CH_{3,\ Cym\text{-}g}$); 0.94 (d, $^3J_{H,H}$ = 7 Hz, 3H, $CH_{3,\ Cym\text{-}g}$) ppm. ^{13}C NMR ($CDCl_3$, 125.75 MHz, 298.5 K): δ = 167.1 ($C_{Ph\text{-}3'}$); 156.2 ($C_{Trz\text{-}4}$); 140.7 ($CH_{Ph\text{-}3'}$); 136.0 ($C_{Ph\text{-}1'}$); 134.1 ($C_{Bn\text{-}1''}$); 129.4 ($CH_{Bn\text{-}3''/5''}$); 129.3 ($CH_{Ph\text{-}4'}$*, $CH_{Bn\text{-}4''}$*); 129.2 ($CH_{Ph\ 4'}$*, $CH_{Bn\ 4''}$*); 129.0 ($CH_{Bn\text{-}2''/6''}$); 125.4 ($CH_{Ph\text{-}5'}$); 124.3 ($CH_{Ph\text{-}6'}$); 120.6 ($CH_{Trz\text{-}5}$); 116.8 ($C_{Cym\text{-}e}$); 108.3 ($C_{Cym\text{-}b}$); 93.6 ($CH_{Cym\text{-}c}$); 91.6 ($CH_{Cym\text{-}d}$); 91.1 ($CH_{Cym\text{-}c}$); 90.2 ($CH_{Cym\text{-}d}$); 56.4 ($CH_{2,\ Bn}$); 46.6 ($CH_{3,\ DMSO}$); 46.0 ($CH_{3,\ DMSO}$); 31.0 ($CH_{Cym\text{-}f}$); 22.7 ($CH_{3,\ Cym\text{-}g}$); 21.7 ($CH_{3,\ Cym\text{-}g}$); 18.9 ($CH_{3,\ Cym\text{-}a}$) ppm. (*): indistinguishable.

*[(κS-Dimethyl sulfoxide) (methyl-2″-(4-(2′-κC)-phenyl-1,2,3-(3-κN)-triazol-1-ylato)acetato)(η⁶-p-cymene)ruthenium(II)] trifluoromethanesulfonate (**2e′**).* The reaction was performed according to the general procedure for the synthesis of DMSO adducts, using **2e** (100 mg, 0.21 mmol), DMSO (30 μL, 0.42 mmol, 2.0 equiv) and AgOTf (106 mg, 0.42 mmol). Yield: 107 mg, 77%. ESI-HR-MS^+ *m/z* Found (Calculated): $[M-DMSO]^+$ 452.0915 (452.0912), $[M]^+$ 530.1058 (530.1051). Elemental Anal. Calc. for $C_{24}H_{30}F_3N_3O_6RuS_2$: C 42.47, H 4.46, N 6.19, S 9.45; Found: C 42.19, H 4.38, N 6.08, S 9.22. ^1H NMR ($CDCl_3$, 500.10 MHz, 298.2 K): δ = 8.42 (s, 1H, $ArH_{Trz\text{-}5}$); 7.94−7.90 (m, 1H, $ArH_{Ph\text{-}3'}$); 7.55 (dd, $^3J_{H,H}$ = 7 Hz, $^4J_{H,H}$ = 2 Hz, 1H, Ar$^3J_{H,H}$ = 7 Hz$^3J_{H,H}$ = 7 Hz$^3J_{H,H}$ = 7 Hz$^3J_{H,H}$ = 7 Hz$^2J_{H,H}$ = 18 Hz$^2J_{H,H}$ = 18 Hz$^3J_{H,H}$ = 7 Hz$^3J_{H,H}$ = 7 Hzd, $^3J_{H,H}$ = 7 Hz^{13}C NMR ($CDCl_3$, 125.75 MHz, 298.5 K): δ = 167.1 (CO_{Ac}*, $C_{Ph\text{-}2'}$*); 156.0 ($C_{Trz\text{-}4}$); 140.6 ($CH_{Ph\text{-}3'}$); 135.9 ($C_{Ph\text{-}1'}$); 129.4 ($CH_{Ph\text{-}4'}$); 125.6 ($CH_{Ph\text{-}5'}$); 124.4 ($CH_{Ph\text{-}6'}$); 122.6 ($CH_{Trz\text{-}5}$); 116.5 ($C_{Cym\text{-}e}$); 109.2 ($C_{Cym\text{-}b}$); 93.3 ($CH_{Cym\text{-}d}$); 91.4 ($CH_{Cym\text{-}c}$); 91.0 ($CH_{Cym\text{-}c}$); 90.8 ($CH_{Cym\text{-}d}$); 53.4 ($OCH_{3,\ Ac}$); 52.7 ($CH_{2,\ Ac}$); 46.4 ($CH_{3,\ DMSO}$); 46.0 ($CH_{3,\ DMSO}$); 31.0 ($CH_{Cym\text{-}f}$); 22.5 ($CH_{3,\ Cym\text{-}g}$); 22.1 ($CH_{3,\ Cym\text{-}g}$); 18.9 ($CH_{3,\ Cym\text{-}a}$) ppm. (*) indistinguishable.

[(κS-Dimethyl sulfoxide) (methyl-2″-(4-(2′-κC)-phenyl-1,2,3-(3-κN)-triazol-1-ylato)acetato)(η⁶-p-cymene)osmium(II)] trifluorome-

DOI: 10.1021/acs.inorgchem.6b02430
Inorg. Chem. XXXX, XXX, XXX−XXX

*thanesulfonate (**3e′**).* The reaction was performed according to the general leaving group exchange procedure, using **3e** (100 mg, 0.17 mmol), DMSO (25 μL, 0.35 mmol) and AgOTf (90 mg, 0.35 mmol). Yield: 98 mg, 73%. ESI-HR-MS$^+$ *m*/*z* Found (Calculated): [M−DMSO]$^+$ 542.1479 (542.1478), [M]$^+$ 620.1620 (620.1616). Elemental Anal. Calc. for $C_{24}H_{30}F_3N_3O_6OsS_2$: C 37.54, H 3.94, N 5.47, S 8.35; Found: C37.46, H 3.96, N 5.38, S 8.28. ^{1}H NMR ($CDCl_3$, 500.10 MHz, 298.2 K): δ = 8.48 (s, 1H, $ArH_{Trz\text{-}5}$); 7.86−7.83 (m, 1H, $ArH_{Ph\text{-}3'}$); 7.60−7.56 (m, 1H, $ArH_{Ph\text{-}6'}$); 7.20−7.13 (m, 2H, $ArH_{Ph\text{-}4'}$, $ArH_{Ph\text{-}5'}$); 5.90−5.86 (m, 2H, $ArH_{Cym\text{-}c}$, $ArH_{Cym\text{-}d}$); 5.70 (d, $^3J_{H,H}$ = 6 Hz, 1H $ArH_{Cym\text{-}d}$); 5.60 (d, $^2J_{H,H}$ = 18 Hz, 1H, $CH_{2,\ Ac}$); 5.56 (d, $^3J_{H,H}$ = 6 Hz, 1H, $ArH_{Cym\text{-}c}$); 5.53 (d, $^2J_{H,H}$ = 18 Hz, 1H, $CH_{2,\ Ac}$); 3.83 (s, 3H, $OCH_{3,\ Ac}$); 2.77 (sept, $^3J_{H,H}$ = 7 Hz, 1H, $CH_{Cym\text{-}f}$); 2.52 (s, 3H, $CH_{3,\ DMSO}$); 2.49 (s, 3H, $CH_{3,\ DMSO}$); 2.33 (s, 3H, $CH_{3,\ DMSO}$); 1.12 (d, $^3J_{H,H}$ = 7 Hz, 3H, $CH_{3,\ Cym\text{-}g}$), 1.03 (d, $^3J_{H,H}$ = 7 Hz, 3H, $CH_{3,\ Cym\text{-}g}$) ppm. ^{13}C NMR ($CDCl_3$, 125.75 MHz, 298.5 K): δ = 167.1 (CO_{Ac}); 158.0 ($C_{Trz\text{-}4}$); 152.3 ($C_{Ph\text{-}2'}$); 140.5 ($CH_{Ph\text{-}3'}$); 136.3 ($C_{Ph\text{-}1'}$); 130.0 ($CH_{Ph\text{-}4'}$); 125.4 ($CH_{Ph\text{-}5'}$); 124.0 ($CH_{Ph\text{-}6'}$); 122.9 ($CH_{Trz\text{-}5}$); 110.5 ($C_{Cym\text{-}e}$); 103.2 ($C_{Cym\text{-}b}$); 83.3 ($CH_{Cym\text{-}c}$); 83.0 ($CH_{Cym\text{-}d}$); 82.4 ($CH_{Cym\text{-}c}$); 82.0 ($CH_{Cym\text{-}d}$); 53.4 ($OCH_{3,\ Ac}$); 52.7 ($CH_{2,\ Ac}$); 47.1 ($CH_{3,\ DMSO}$); 44.2 ($CH_{3,\ DMSO}$); 30.7 ($CH_{Cym\text{-}f}$); 22.8 ($CH_{3,\ Cym\text{-}g}$); 22.2 ($CH_{3,\ Cym\text{-}g}$); 18.7 ($CH_{3,\ Cym\text{-}a}$) ppm.

Stability in aqueous solution by UV−vis spectroscopy. Stock solutions (2 mM) of complexes in DMSO or DMF were prepared, diluted with phosphate buffer (67 mM, pH 7.4) to a concentration of 20 μM in 1% DMSO or DMF/buffer, filtered, and UV−vis spectra recorded in 15 min intervals for 24 h at 25 °C on a PerkinElmer *Lambda 35* UV−vis spectrophotometer.

Stability in aqueous solution and amino acid binding studies by ESI-MS. Stock solutions of complexes in DMSO or DMF were prepared and diluted to concentration of 5 μM complex in 1% DMSO or DMF in 400 μM ammonium acetate solution (pH 7.4) or water. For competitive amino acid binding experiments, complex stock solutions were incubated with 400 μM ammonium acetate solution (pH 7.4) containing 5 μM L-cysteine, L-histidine, and L-methionine. Aliquots were taken after 0, 1, 3, 6, and 24 h of incubation at 37 °C and stored at −20 °C until analysis. Electrospray ionization mass spectra of the collected samples were recorded on a Bruker AmaZon SL ion trap mass spectrometer by direct infusion after dilution with methanol (1:1).

Aquation-anation equilibrium by NMR spectroscopy. Stock solutions of **2e** and **3e** in d_7-DMF (5 mM) were diluted to a final concentration of 500 μM with pure D_2O, or D_2O containing 5 mM and 154 mM NaCl respectively, whereupon NMR spectra acquisition was started as fast as possible (~3.5 min after sample preparation). To test the reversibility of aquation, a 500 μM solution of **2e** prepared as described above was allowed to fully hydrolyze for 30 min, then appropriate amounts of solid NaCl were added to an overall concentrations of 5 mM, 154 mM and 1 M and NMR spectra measured.

Stability toward aqueous phosphate buffers by NMR spectroscopy. Stock solutions (5 mM) of **2e** and **3e** in d_6-DMSO and d_7-DMF respectively were diluted with D_2O containing a 12 mM phosphate buffer at pD 7.9 (equals pH 7.4)[69] to 10% DMF/DMSO in D_2O. Subsequently, ^{1}H and ^{31}P NMR spectra were recorded over 24 h.

Single crystal X-ray diffraction analysis. The X-ray intensity data was measured on a Bruker *D8-Venture* or a Bruker *X8-APEX2* diffractometer equipped with multilayer monochromators, Mo K/a INCOATEC micro focus sealed tubes (λ_{Mo} = 0.71073 Å) and Kryoflex cooling devices. All samples were uploaded to the CCDC, for CCDC codes see Table S1. The structures were solved by either direct methods or charge flipping, and refined by full-matrix least-squares techniques. Non-hydrogen atoms were refined with anisotropic displacement parameters. Hydrogen atoms were inserted in calculated positions and refined with a riding model as rotating systems. The following software was used: Frame integration - *Bruker SAINT software package*[70] using a narrow-frame algorithm; Absorption correction - *SADABS*;[71] structure solution - *SHELXS-97*;[72] refinement - *SHELXL-2014*,[73] *OLEX2*,[74] *SHELXLE*;[75] molecular diagrams - *OLEX2*.[74] Experimental parameters can be found in Table S1. Crystal data, data collection parameters, and structure refinement details are given in Tables S10−S29. Molecular Structures in "Ortep View" are given in Figure S5−S14. A tabular overview for half sandwich structure parameters is given in Table S2. The parameters for $\pi-\pi$ and $\sigma-\pi$ interactions and their graphical representation can be found in Table S7−S9 and Figure S4 respectively. Disordered moieties are excluded from detailed analysis in all tables listing structural parameters, due to constraints and restraints.

cLog*P* calculation. The octanol−water partition coefficient Log*P* was calculated for the free ligands with Molinspiration (v2014.11). The cLog*P* values allow the comparison of relative lipophilicities within a series of osmium(II)- or ruthenium(II)-arene metalacycles, as the metal-arene fragments remain unchanged and should add a constant contribution to the overall lipophilicity, while the ligands are varied.

Cell culture. CH1/PA-1 (kindly provided by Lloyd R. Kelland, CRC Centre for Cancer Therapeutics, Institute of Cancer Research, Sutton, UK; identified through STR profiling as PA-1 ovarian teratocarcinoma cells[76] by Multiplexion, Heidelberg, Germany), SW480 (colon carcinoma; from ATCC) and A549 (non-small cell lung cancer; from ATCC) cells were grown as adherent monolayer cultures in 75 cm^2 culture flasks (Starlab, UK) in minimal essential medium (MEM; Sigma-Aldrich) supplemented with 10% heat-inactivated fetal bovine serum (Invitrogen or Biowest), 1 mM sodium pyruvate, 4 mM L-glutamine, and 1% non-essential amino acids from 100× ready-to-use stock solution (all purchased from Sigma-Aldrich). Cell cultures were incubated at 37 °C in a moist atmosphere containing 5% CO_2 in air.

MTT assay. The cytotoxicity of the compounds was determined by the colorimetric MTT assay (MTT = 3-(4,5-dimethyl-2-thiazolyl)-2,5-diphenyl-2*H*-tetrazolium bromide). For this purpose, cells were harvested from culture flasks by trypsinization, seeded in 100 μL aliquots into 96-well microculture plates (Starlab, UK) in densities of 1 × 10^3 (CH1/PA-1), 2 × 10^3 (SW480) and 3 × 10^3 (A549) cells per well, and incubated for 24 h prior to exposure to the test compounds. Stock solutions of test compounds were prepared in DMSO or DMF, which were then diluted in MEM (not to exceed a final content of 0.5% v/v of organic solvent in the test plates), and serial dilutions were added in aliquots of 100 μL per well. After continuous exposure for 96 h, drug solutions were replaced with 100 μL medium/MTT mixtures [6 parts of RPMI 1640 medium supplemented with 10% heat-inactivated fetal bovine serum and 2 mM L-glutamine; 1 part of MTT solution in phosphate-buffered saline (5 mg/mL)]. After incubation for 4 h, the medium/MTT mixtures were removed, and the produced formazan crystals were dissolved in 150 μL DMSO per well.

Optical densities at 550 nm were measured spectrophotometrically (ELx808 Absorbance Microplate Reader, Bio-Tek, USA) by using a reference wavelength of 690 nm to correct for unspecific absorption. 50% inhibitory concentrations (IC_{50}) were calculated from concentration−effect curves by interpolation based on at least three independent experiments, each comprising triplicates per concentration level.

Cellular accumulation. Cellular accumulation of the compounds was studied based on a method described previously[77] with minor modifications. 1.2 × 10^5 SW480 cells per well were seeded into six-well plates in aliquots of 2.5 mL complete MEM (see above) and incubated at 37 °C for 24 h. Then, cells were exposed for 2 h at 37 °C to 50 μM solutions of the test compounds (containing 0.5% DMSO) in fresh 2.5 mL of complete MEM upon exchange of the medium. Afterward, cells were washed three times with PBS, and lysed with 0.4 mL subboiled HNO_3 per well for 1 h at room temperature. Ruthenium content was quantified by inductively coupled plasma mass spectrometry (ICP-MS) using an ICP-quadrupole MS Agilent 7500ce instrument (Agilent Technologies, Waldbronn, Germany) equipped with a CETAX ASX-520 autosampler (Nebraska, USA) and a MicroMist nebulizer. Ruthenium and indium standards were obtained from CPI International (Amsterdam, The Netherlands). The instrument was equipped with nickel cones and operated at an RF power of 1560 W, with argon as the plasma gas (15 L min^{-1}), carrier gas (1.0−1.1 L min^{-1}) and

DOI: 10.1021/acs.inorgchem.6b02430
Inorg. Chem. XXXX, XXX, XXX−XXX

make up gas (0.1−0.2 L min^{-1}). The Agilent MassHunter software package (Workstation Software, Version B.01.01, Build 123.11, Patch 4, 2012) was used for data processing. Adsorption/desorption blank data were subtracted from the data for the corresponding accumulation sample, and the ruthenium content is given relative to the cell number. Results are based on three independent experiments, each comprising triplicate samples. Monitored isotopes were ^{101}Ru, ^{102}Ru and ^{115}In, the latter is being used as internal standard. The ICP-MS was tuned on a daily basis to achieve maximum sensitivity.

Topoisomerase IIα assay. Topoisomerase IIα inhibition experiments were conducted with a topoisomerase II drug screening kit from Enzo Life Sciences according to the manufacturer guidelines. First, two 1% agarose gels were prepared, one containing 0.75 μg/mL EtBr and the other without EtBr. All test compounds were dissolved and diluted in DMF so that a maximum of 0.625% DMF was loaded onto the gel, while **2b** was additionally dissolved and diluted in DMSO to a final concentration of 0.08% DMSO in the gel. 800 μM etoposide (VP-16) was used as a positive control. Linear DNA was used as a marker and 0.625% DMF was used as a solvent control. DMSO was previously shown to not inhibit topoisomerase IIα in the used concentrations.[65] Two mastermixes were prepared, the first containing 10 μL water and 1 μL DNA per reaction and the second containing 1 μL topoisomerase IIα and 2 μL buffer A and 2 μL buffer B per reaction. Reaction tubes were incubated at 37 °C for 30 min. The compound was added in 4 μL of water, the final reaction volume was 20 μL. Reaction was stopped by using 2 μL 10% SDS. Afterward, proteinase K was added to digest the enzyme at 37 °C for 15 min. Then loading dye was added and each sample split in two. Half of the sample was loaded onto the EtBr containing gel, the other half was loaded onto the other agarose gel. Gels were run with 60 V until they reached 30% of the gel and then voltage was increased to 80 V until the staining front reached the edge of the gel. The EtBr containing gel was washed for 20 min in running buffer. The other gel was stained for 20 min in running buffer containing 0.75 μg/mL EtBr. Pictures were taken by using a Fusion FX7 system (Vilber Lourmat, Germany). Two independent experiments were performed.

Cell cycle analysis. 6 ×10^4 cells (SW480 cell line) were seeded into 24-well plates and allowed to adhere for 24 h at 37 °C under 5% CO_2 before treatment. Cells were treated with indicated concentrations for 48 h at 37 °C under 5% CO_2. For this purpose, the test substances were dissolved in DMF and diluted to different concentrations in MEM. Positive controls were 0.01 μM and 0.05 μM gemcitabine. After treatment the cells were viable and 80−90% confluent. Cells were washed once with PBS, detached by using 150 μL trypsin-EDTA. After trypsinization was stopped by adding 850 μL of MEM, cells were collected in microreaction tubes and centrifuged at 300g at RT for 3 min. Supernatants were discarded and cells washed once with 1 mL PBS. Cells were then resuspended in 300 μL PI/HSF solution (50 μg/mL) and stained overnight. Measurement was performed on a Guava easyCyte flow cytometer (Millipore). Cells were sorted by forward and side scatter and the red fluorescence measured dependent on the cell number. At least three independent experiments were performed. Analysis was performed by using the cell cycle function in FlowJo software (TreeStar, Inc., Ashland, OR, USA).

■ ASSOCIATED CONTENT

Supporting Information

The Supporting Information is available free of charge on the ACS Publications website at DOI: 10.1021/acs.inorgchem.6b02430.

Synthesis and characterization of ligands **1a−e**; X-ray diffraction experimental and acquisition parameters; CCDC codes; geometry parameters; crystal structures in ORTEP view; sample and crystal data; data collection and refinement parameters; UV−vis stability spectra; ESI-MS stability and amino acid interaction spectra of **2a**; aquation−anation curve of **3e**; topoisomerase IIα screening assay; cell cycle distribution after treatment with **1e**, **2e**, and **3e**; ^1H and ^{13}C NMR spectra of **2a−e**, **3a−e**, **2a′**, **2e′**, and **3e′** (PDF)

Crystallographic data for **2a−e** and **3a−e** (CIF)

■ AUTHOR INFORMATION

Corresponding Author

*E-mail: wolfgang.kandioller@univie.ac.at; Tel: +43-1-4277-52609; Fax: +43-1-4277-9526.

ORCID

Wolfgang Kandioller: 0000-0002-5630-712X

Notes

The authors declare no competing financial interest.

■ ACKNOWLEDGMENTS

We thank the University of Vienna for financial support.

■ REFERENCES

(1) Hartinger, C. G.; Zorbas-Seifried, S.; Jakupec, M. A.; Kynast, B.; Zorbas, H.; Keppler, B. K. From Bench to Bedside − Preclinical and Early Clinical Development of the Anticancer Agent Indazolium Trans-[tetrachlorobis(1H-indazole)ruthenate(III)] (KP1019 or FFC14A). *J. Inorg. Biochem.* **2006**, *100*, 891−904.

(2) Thompson, D. S.; Weiss, G. J.; Jones, S. F.; Burris, H. A.; Ramanathan, R. K.; Infante, J. R.; Bendell, J. C.; Ogden, A.; Von Hoff, D. D. NKP1339 Phase I Trial. *J. Clin. Oncol.* **2012**, *30* (*Suppl.*), Abstr. 3033.

(3) Jakupec, M. A.; Reisner, E.; Eichinger, A.; Pongratz, M.; Arion, V. B.; Galanski, M.; Hartinger, C. G.; Keppler, B. K. Redox-Active Antineoplastic Ruthenium Complexes with Indazole: Correlation of in Vitro Potency and Reduction Potential. *J. Med. Chem.* **2005**, *48*, 2831−2837.

(4) Aird, R. E.; Cummings, J.; Ritchie, A. A.; Muir, M.; Morris, R. E.; Chen, H.; Sadler, P. J.; Jodrell, D. I. In Vitro and in Vivo Activity and Cross Resistance Profiles of Novel Ruthenium (II) Organometallic Arene Complexes in Human Ovarian Cancer. *Br. J. Cancer* **2002**, *86*, 1652−1657.

(5) Scolaro, C.; Bergamo, A.; Brescacin, L.; Delfino, R.; Cocchietto, M.; Laurenczy, G.; Geldbach, T. J.; Sava, G.; Dyson, P. J. In Vitro and in Vivo Evaluation of Ruthenium(II)−Arene PTA Complexes. *J. Med. Chem.* **2005**, *48*, 4161−4171.

(6) Kilpin, K. J.; Dyson, P. J. Enzyme Inhibition by Metal Complexes: Concepts, Strategies and Applications. *Chem. Sci.* **2013**, *4*, 1410−1419.

(7) Schmid, W. F.; John, R. O.; Mühlgassner, G.; Heffeter, P.; Jakupec, M. A.; Galanski, M.; Berger, W.; Arion, V. B.; Keppler, B. K. Metal-Based Paullones as Putative CDK Inhibitors for Antitumor Chemotherapy. *J. Med. Chem.* **2007**, *50*, 6343−6355.

(8) Kurzwernhart, A.; Kandioller, W.; Bartel, C.; Bächler, S.; Trondl, R.; Mühlgassner, G.; Jakupec, M. A.; Arion, V. B.; Marko, D.; Keppler, B. K.; Hartinger, C. G. Targeting the DNA-Topoisomerase Complex in a Double-Strike Approach with a Topoisomerase Inhibiting Moiety and Covalent DNA Binder. *Chem. Commun.* **2012**, *48*, 4839−4841.

(9) Kubanik, M.; Kandioller, W.; Kim, K.; Anderson, R. F.; Klapproth, E.; Jakupec, M. A.; Roller, A.; Söhnel, T.; Keppler, B. K.; Hartinger, C. G. Towards targeting anticancer drugs: ruthenium(II)−arene complexes with biologically active naphthoquinone-derived ligand systems. *Dalton Trans.* **2016**, *45*, 13091−13103.

(10) Wang, F.; Habtemariam, A.; van der Geer, E. P.; Fernández, R.; Melchart, M.; Deeth, R. J.; Aird, R.; Guichard, S.; Fabbiani, F. P.; Lozano-Casal, P.; et al. Controlling Ligand Substitution Reactions of Organometallic Complexes: Tuning Cancer Cell Cytotoxicity. *Proc. Natl. Acad. Sci. U. S. A.* **2005**, *102*, 18269−18274.

(11) Kandioller, W.; Hartinger, C. G.; Nazarov, A. A.; Kuznetsov, M. L.; John, R. O.; Bartel, C.; Jakupec, M. A.; Arion, V. B.; Keppler, B. K. From Pyrone to Thiopyrone Ligands−Rendering Maltol-Derived Ruthenium(II)−Arene Complexes That Are Anticancer Active in Vitro. *Organometallics* **2009**, *28*, 4249−4251.

DOI: 10.1021/acs.inorgchem.6b02430
Inorg. Chem. XXXX, XXX, XXX−XXX

(12) Kasser, J. H.; Kandioller, W.; Hartinger, C. G.; Nazarov, A. A.; Arion, V. B.; Dyson, P. J.; Keppler, B. K. Mannich Products of Kojic Acid and N-Heterocycles and Their Ru(II)−arene Complexes: Synthesis, Characterization and Stability. *J. Organomet. Chem.* **2010**, *695*, 875−881.
(13) Schmidlehner, M.; Pichler, V.; Roller, A.; Jakupec, M. A.; Kandioller, W.; Keppler, B. K. Organometallic Complexes of (Thio)allomaltol-Based Mannich-Products: Synthesis, Stability and Preliminary Biological Investigations. *J. Organomet. Chem.* **2015**, *782*, 69−76.
(14) Martínez-Alonso, M.; Busto, N.; Jalón, F. A.; Manzano, B. R.; Leal, J. M.; Rodríguez, A. M.; García, B.; Espino, G. Derivation of Structure−Activity Relationships from the Anticancer Properties of Ruthenium(II) Arene Complexes with 2-Aryldiazole Ligands. *Inorg. Chem.* **2014**, *53*, 11274−11288.
(15) Belsa, L.; López, C.; González, A.; Font-Bardía, M.; Calvet, T.; Calvis, C.; Messeguer, R. Neutral and Ionic Cycloruthenated 2-Phenylindoles as Cytotoxic Agents. *Organometallics* **2013**, *32*, 7264−7267.
(16) Ruiz, J.; Rodríguez, V.; Cutillas, N.; Espinosa, A.; Hannon, M. J. A Potent Ruthenium(II) Antitumor Complex Bearing a Lipophilic Levonorgestrel Group. *Inorg. Chem.* **2011**, *50*, 9164−9171.
(17) Yellol, J.; Pérez, S. A.; Buceta, A.; Yellol, G.; Donaire, A.; Szumlas, P.; Bednarski, P. J.; Makhloufi, G.; Janiak, C.; Espinosa, A.; Ruiz, J. Novel C,N-Cyclometalated Benzimidazole Ruthenium(II) and Iridium(III) Complexes as Antitumor and Antiangiogenic Agents: A Structure−Activity Relationship Study. *J. Med. Chem.* **2015**, *58*, 7310−7327.
(18) Yellol, G. S.; Donaire, A.; Yellol, J. G.; Vasylyeva, V.; Janiak, C.; Ruiz, J. On the Antitumor Properties of Novel Cyclometalated Benzimidazole Ru(II), Ir(III) and Rh(III) Complexes. *Chem. Commun.* **2013**, *49*, 11533−11535.
(19) Ferrer Flegeau, E.; Bruneau, C.; Dixneuf, P. H.; Jutand, A. Autocatalysis for C−H Bond Activation by Ruthenium(II) Complexes in Catalytic Arylation of Functional Arenes. *J. Am. Chem. Soc.* **2011**, *133*, 10161−10170.
(20) Fabre, I.; von Wolff, N.; Le Duc, G.; Ferrer Flegeau, E.; Bruneau, C.; Dixneuf, P. H.; Jutand, A. Autocatalytic Intermolecular versus Intramolecular Deprotonation in C-H Bond Activation of Functionalized Arenes by Ruthenium(II) or Palladium(II) Complexes. *Chem. - Eur. J.* **2013**, *19*, 7595−7604.
(21) Ryabov, A. D.; Soukharev, V. S.; Alexandrova, L.; Le Lagadec, R.; Pfeffer, M. Low-Potential Cyclometalated Osmium(II) Mediators of Glucose Oxidase. *Inorg. Chem.* **2003**, *42*, 6598−6600.
(22) Cerón-Camacho, R.; Morales-Morales, D.; Hernandez, S.; Le Lagadec, R.; Ryabov, A. D. Easy Access to Bio-Inspired Osmium(II) Complexes through Electrophilic Intramolecular C(sp2)-H Bond Cyclometalation. *Inorg. Chem.* **2008**, *47*, 4988−4995.
(23) Cerón-Camacho, R.; Hernández, S.; Le Lagadec, R.; Ryabov, A. D. Cyclometalated [Os(C−N)x(N−N)3−x]m+ Mimetics of tris(2,2′-Bipyridine)osmium(II): Covering a 2 V Potential Range by Known (X = 0, 1) and New (X = 2, 3) Species (C−N = O-2-Phenylpyridinato). *Chem. Commun.* **2011**, *47*, 2823−2825.
(24) Bolje, A.; Hohloch, S.; van der Meer, M.; Košmrlj, J.; Sarkar, B. RuII, OsII, and IrIII Complexes with Chelating Pyridyl−Mesoionic Carbene Ligands: Structural Characterization and Applications in Transfer Hydrogenation Catalysis. *Chem. - Eur. J.* **2015**, *21*, 6756−6764.
(25) Boff, B.; Gaiddon, C.; Pfeffer, M. Cancer Cell Cytotoxicity of Cyclometalated Compounds Obtained with Osmium(II) Complexes. *Inorg. Chem.* **2013**, *52*, 2705−2715.
(26) Rostovtsev, V. V.; Green, L. G.; Fokin, V. V.; Sharpless, K. B. A Stepwise Huisgen Cycloaddition Process: Copper(I)-Catalyzed Regioselective "Ligation" of Azides and Terminal Alkynes. *Angew. Chem., Int. Ed.* **2002**, *41*, 2596−2599.
(27) Tornøe, C. W.; Christensen, C.; Meldal, M. Peptidotriazoles on Solid Phase: [1,2,3]-Triazoles by Regiospecific Copper(I)-Catalyzed 1,3-Dipolar Cycloadditions of Terminal Alkynes to Azides. *J. Org. Chem.* **2002**, *67*, 3057−3064.
(28) Liang, L.; Astruc, D. The copper(I)-Catalyzed Alkyne-Azide Cycloaddition (CuAAC) "click" Reaction and Its Applications. An Overview. *Coord. Chem. Rev.* **2011**, *255*, 2933−2945.
(29) Dalvie, D. K.; Kalgutkar, A. S.; Khojasteh-Bakht, S. C.; Obach, R. S.; O'Donnell, J. P. Biotransformation Reactions of Five-Membered Aromatic Heterocyclic Rings. *Chem. Res. Toxicol.* **2002**, *15*, 269−299.
(30) Elliott, P. I. P. Organometallic Complexes with 1,2,3-Triazole-Derived Ligands. In *Organometallic Chemistry*; Fairlamb, I. J. S., Lynam, J. M., Eds.; Royal Society of Chemistry: Cambridge, 2014; Vol. *39*, Chapter 1; pp 1−25.
(31) Mathew, P.; Neels, A.; Albrecht, M. 1,2,3-Triazolylidenes as Versatile Abnormal Carbene Ligands for Late Transition Metals. *J. Am. Chem. Soc.* **2008**, *130*, 13534−13535.
(32) Mercs, L.; Albrecht, M. Beyond Catalysis: N-Heterocyclic Carbene Complexes as Components for Medicinal, Luminescent, and Functional Materials Applications. *Chem. Soc. Rev.* **2010**, *39*, 1903−1912.
(33) Donnelly, K. F.; Petronilho, A.; Albrecht, M. Application of 1,2,3-Triazolylidenes as Versatile NHC-Type Ligands: Synthesis, Properties, and Application in Catalysis and beyond. *Chem. Commun.* **2013**, *49*, 1145−1159.
(34) Hohloch, S.; Suntrup, L.; Sarkar, B. Arene−Ruthenium(II) and − Iridium(III) Complexes with "Click"-Based Pyridyl-Triazoles, Bis-Triazoles, and Chelating Abnormal Carbenes: Applications in Catalytic Transfer Hydrogenation of Nitrobenzene. *Organometallics* **2013**, *32*, 7376−7385.
(35) Bratsos, I.; Urankar, D.; Zangrando, E.; Genova-Kalou, P.; Košmrlj, J.; Alessio, E.; Turel, I. 1-(2-Picolyl)-Substituted 1,2,3-Triazole as Novel Chelating Ligand for the Preparation of Ruthenium Complexes with Potential Anticancer Activity. *Dalton Trans.* **2011**, *40*, 5188−5199.
(36) Felici, M.; Contreras-Carballada, P.; Vida, Y.; Smits, J. M. M.; Nolte, R. J. M.; De Cola, L.; Williams, R. M.; Feiters, M. C. IrIII and RuII Complexes Containing Triazole-Pyridine Ligands: Luminescence Enhancement upon Substitution with β-Cyclodextrin. *Chem. - Eur. J.* **2009**, *15*, 13124−13134.
(37) Welby, C. E.; Grkinic, S.; Zahid, A.; Uppal, B. S.; Gibson, E. A.; Rice, C. R.; Elliott, P. I. P. Synthesis, Characterisation and Theoretical Study of Ruthenium 4,4′-Bi-1,2,3-Triazolyl Complexes: Fundamental Switching of the Nature of S1 and T1 States from MLCT to MC. *Dalton Trans.* **2012**, *41*, 7637−7646.
(38) Mattiuzzi, A.; Jabin, I.; Moucheron, C.; Kirsch-De Mesmaeker, A. Ru-TAP Complexes with Btz and Pytz Ligands: Novel Candidates as Photooxidizing Agents. *Dalton Trans.* **2011**, *40*, 7395−7402.
(39) Obata, M.; Kitamura, A.; Mori, A.; Kameyama, C.; Czaplewska, J. A.; Tanaka, R.; Kinoshita, I.; Kusumoto, T.; Hashimoto, H.; Harada, M.; Mikata, Y.; Funabiki, T.; Yano, S. Syntheses, Structural Characterization and Photophysical Properties of 4-(2-Pyridyl)-1,2,3-Triazole Rhenium(I) Complexes. *Dalton Trans.* **2008**, *25*, 3292−3300.
(40) Zanarini, S.; Felici, M.; Valenti, G.; Marcaccio, M.; Prodi, L.; Bonacchi, S.; Contreras-Carballada, P.; Williams, R. M.; Feiters, M. C.; Nolte, R. J. M.; De Cola, L.; Paolucci, F. Green and Blue Electrochemically Generated Chemiluminescence from Click Chemistry—Customizable Iridium Complexes. *Chem. - Eur. J.* **2011**, *17*, 4640−4647.
(41) Yang, W.; Zhong, Y. Cyclometalated Ruthenium Complexes of 1,2,3-Triazole-Containing Ligands: Synthesis, Structural Studies, and Electronic Properties. *Chin. J. Chem.* **2013**, *31*, 329−338.
(42) Beyer, B.; Ulbricht, C.; Escudero, D.; Friebe, C.; Winter, A.; González, L.; Schubert, U. S. Phenyl-1H-[1,2,3]triazoles as New Cyclometalating Ligands for Iridium(III) Complexes. *Organometallics* **2009**, *28*, 5478−5488.
(43) Bagh, B.; McKinty, A. M.; Lough, A. J.; Stephan, D. W. 1,2,3-Triazolylidene ruthenium(II)(η6-Arene) Complexes: Synthesis, Metallation and Reactivity. *Dalton Trans.* **2014**, *43*, 12842−12850.
(44) Ogata, K.; Inomata, S.; Fukuzawa, S. Position-Selective Intramolecular Aromatic C−H Bond Activation of 1,2,3-Triazol-5-Ylidene (tzNHC) Ligands in (*p*-cymene)ruthenium(II) Complexes. *Dalton Trans.* **2013**, *42*, 2362−2365.

DOI: 10.1021/acs.inorgchem.6b02430
Inorg. Chem. XXXX, XXX, XXX−XXX

(45) Bolje, A.; Hohloch, S.; Urankar, D.; Pevec, A.; Gazvoda, M.; Sarkar, B.; Košmrlj, J. Exploring the Scope of Pyridyl- and Picolyl-Functionalized 1,2,3-Triazol-5-Ylidenes in Bidentate Coordination to Ruthenium(II) Cymene Chloride Complexes. *Organometallics* **2014**, *33*, 2588−2598.
(46) Bernet, L.; Lalrempuia, R.; Ghattas, W.; Mueller-Bunz, H.; Vigara, L.; Llobet, A.; Albrecht, M. Tunable Single-Site Ruthenium Catalysts for Efficient Water Oxidation. *Chem. Commun.* **2011**, *47*, 8058−8060.
(47) Kumar, S.; Saleem, F.; Singh, A. K. Click" Generated 1,2,3-Triazole Based Organosulfur/Selenium Ligands and Their Pd(II) and Ru(II) Complexes: Their Synthesis, Structure and Catalytic Applications. *Dalton Trans* **2016**, *45*, 11445−11458.
(48) Alvarez, S. G.; Alvarez, M. T. A Practical Procedure for the Synthesis of Alkyl Azides at Ambient Temperature in Dimethyl Sulfoxide in High Purity and Yield. *Synthesis* **1997**, 413−414.
(49) Kolb, H. C.; Finn, M. G.; Sharpless, K. B. Click Chemistry: Diverse Chemical Function from a Few Good Reactions. *Angew. Chem., Int. Ed.* **2001**, *40*, 2004−2021.
(50) Kacprzak, K. Efficient One-Pot Synthesis of 1,2,3-Triazoles from Benzyl and Alkyl Halides. *Synlett* **2005**, 943−946.
(51) Alberico, D.; Scott, M. E.; Lautens, M. Aryl−Aryl Bond Formation by Transition-Metal-Catalyzed Direct Arylation. *Chem. Rev.* **2007**, *107*, 174−238.
(52) Ackermann, L.; Novák, P.; Vicente, R.; Pirovano, V.; Potukuchi, H. Ruthenium-Catalyzed C-H Bond Functionalizations of 1,2,3-Triazol-4-yl-Substituted Arenes: Dehydrogenative Couplings Versus Direct Arylations. *Synthesis* **2010**, *2010*, 2245−2253.
(53) Li, B.; Darcel, C.; Roisnel, T.; Dixneuf, P. H. Cycloruthenation of Aryl Imines and N-Heteroaryl Benzenes via C−H Bond Activation with Ru(II) and Acetate Partners. *J. Organomet. Chem.* **2015**, *793*, 200−209.
(54) Janiak, C. A Critical Account on $\pi-\pi$ Stacking in Metal Complexes with Aromatic Nitrogen-Containing Ligands. *J. Chem. Soc., Dalton Trans.* **2000**, 3885−3896.
(55) Kandioller, W.; Hartinger, C. G.; Nazarov, A. A.; Bartel, C.; Skocic, M.; Jakupec, M. A.; Arion, V. B.; Keppler, B. K. Maltol-Derived Ruthenium−Cymene Complexes with Tumor Inhibiting Properties: The Impact of Ligand−Metal Bond Stability on Anticancer Activity In Vitro. *Chem. - Eur. J.* **2009**, *15*, 12283−12291.
(56) Mokesch, S.; Novak, M. S.; Roller, A.; Jakupec, M. A.; Kandioller, W.; Keppler, B. K. 1,3-Dioxoindan-2-Carboxamides as Bioactive Ligand Scaffolds for the Development of Novel Organometallic Anticancer Drugs. *Organometallics* **2015**, *34*, 848−857.
(57) van Rijt, S. H.; Peacock, A. F. A.; Johnstone, R. D. L.; Parsons, S.; Sadler, P. J. Organometallic Osmium(II) Arene Anticancer Complexes Containing Picolinate Derivatives. *Inorg. Chem.* **2009**, *48*, 1753−1762.
(58) Peacock, A. F. A.; Habtemariam, A.; Fernández, R.; Walland, V.; Fabbiani, F. P. A.; Parsons, S.; Aird, R. E.; Jodrell, D. I.; Sadler, P. J. Tuning the Reactivity of Osmium(II) and Ruthenium(II) Arene Complexes under Physiological Conditions. *J. Am. Chem. Soc.* **2006**, *128*, 1739−1748.
(59) Patra, M.; Joshi, T.; Pierroz, V.; Ingram, K.; Kaiser, M.; Ferrari, S.; Spingler, B.; Keiser, J.; Gasser, G. DMSO-Mediated Ligand Dissociation: Renaissance for Biological Activity of N-Heterocyclic-$[Ru(\eta^6\text{-arene})Cl_2]$ Drug Candidates. *Chem. - Eur. J.* **2013**, *19*, 14768−14772.
(60) Bergamo, A.; Masi, A.; Peacock, A. F. A.; Habtemariam, A.; Sadler, P. J.; Sava, G. In Vivo Tumour and Metastasis Reduction and in Vitro Effects on Invasion Assays of the Ruthenium RM175 and Osmium AFAP51 Organometallics in the Mammary Cancer Model. *J. Inorg. Biochem.* **2010**, *104*, 79−86.
(61) Wang, F.; Chen, H.; Parsons, S.; Oswald, I. D. H.; Davidson, J. E.; Sadler, P. J. Kinetics of Aquation and Anation of Ruthenium(II) Arene Anticancer Complexes, Acidity and X-Ray Structures of Aqua Adducts. *Chem. - Eur. J.* **2003**, *9*, 5810−5820.
(62) Peacock, A. F. A.; Melchart, M.; Deeth, R. J.; Habtemariam, A.; Parsons, S.; Sadler, P. J. Osmium(II) and Ruthenium(II) Arene Maltolato Complexes: Rapid Hydrolysis and Nucleobase Binding. *Chem. - Eur. J.* **2007**, *13*, 2601−2613.
(63) Varbanov, H. P.; Göschl, S.; Heffeter, P.; Theiner, S.; Roller, A.; Jensen, F.; Jakupec, M. A.; Berger, W.; Galanski, M.; Keppler, B. K. A Novel Class of Bis- and Tris-Chelate Diam(m)inebis(dicarboxylato)-platinum(IV) Complexes as Potential Anticancer Prodrugs. *J. Med. Chem.* **2014**, *57*, 6751−6764.
(64) Kurzwernhart, A.; Kandioller, W.; Bächler, S.; Bartel, C.; Martic, S.; Buczkowska, M.; Mühlgassner, G.; Jakupec, M. A.; Kraatz, H.-B.; Bednarski, P. J.; Arion, V. B.; Marko, D.; Keppler, B. K.; Hartinger, C. G. Structure−Activity Relationships of Targeted Ru(II) (η^6-*p*-Cymene) Anticancer Complexes with Flavonol-Derived Ligands. *J. Med. Chem.* **2012**, *55*, 10512−10522.
(65) Schmidlehner, M.; Flocke, L. S.; Roller, A.; Hejl, M.; Jakupec, M. A.; Kandioller, W.; Keppler, B. K. Cytotoxicity and Preliminary Mode of Action Studies of Novel 2-Aryl-4-Thiopyrone-Based Organometallics. *Dalton Trans.* **2016**, *45*, 724−733.
(66) Fulmer, G. R.; Miller, A. J. M.; Sherden, N. H.; Gottlieb, H. E.; Nudelman, A.; Stoltz, B. M.; Bercaw, J. E.; Goldberg, K. I. NMR Chemical Shifts of Trace Impurities: Common Laboratory Solvents, Organics, and Gases in Deuterated Solvents Relevant to the Organometallic Chemist. *Organometallics* **2010**, *29*, 2176−2179.
(67) Bennett, M. A.; Smith, A. K. Arene ruthenium(II) Complexes Formed by Dehydrogenation of Cyclohexadienes with ruthenium(III) Trichloride. *J. Chem. Soc., Dalton Trans.* **1974**, 233−241.
(68) Werner, H.; Zenkert, K. Aromaten(Phosphan)metall-Komplexe. *J. Organomet. Chem.* **1988**, *345*, 151−166.
(69) Krężel, A.; Bal, W. A Formula for Correlating pKa Values Determined in D2O and H2O. *J. Inorg. Biochem.* **2004**, *98* (1), 161−166.
(70) Bruker. *SAINT* V7.68A & V8.32B; Bruker AXS: 2005−2015.
(71) Sheldrick, G. M. SADABS. *Univ. Gött. Ger.* **1996**.
(72) Sheldrick, G. M. A Short History of SHELX. *Acta Crystallogr., Sect. A: Found. Crystallogr.* **2008**, *64*, 112−122.
(73) Sheldrick, G. M. Crystal Structure Refinement with SHELXL. *Acta Crystallogr., Sect. C: Struct. Chem.* **2015**, *C71*, 3−8.
(74) Dolomanov, O. V.; Bourhis, L. J.; Gildea, R. J.; Howard, J. A. K.; Puschmann, H. *OLEX2*: A Complete Structure Solution, Refinement and Analysis Program. *J. Appl. Crystallogr.* **2009**, *42*, 339−341.
(75) Hübschle, C. B.; Sheldrick, G. M.; Dittrich, B. ShelXle: A Qt Graphical User Interface for SHELXL. *J. Appl. Crystallogr.* **2011**, *44*, 1281−1284.
(76) Korch, C.; Spillman, M. A.; Jackson, T. A.; Jacobsen, B. M.; Murphy, S. K.; Lessey, B. A.; Jordan, V. C.; Bradford, A. P. DNA Profiling Analysis of Endometrial and Ovarian Cell Lines Reveals Misidentification, Redundancy and Contamination. *Gynecol. Oncol.* **2012**, *127*, 241−248.
(77) Egger, A. E.; Rappel, C.; Jakupec, M. A.; Hartinger, C. G.; Heffeter, P.; Keppler, B. K. Development of an Experimental Protocol for Uptake Studies of Metal Compounds in Adherent Tumor Cells. *J. Anal. At. Spectrom.* **2009**, *24*, 51−61.

DOI: 10.1021/acs.inorgchem.6b02430
Inorg. Chem. XXXX, XXX, XXX−XXX